Effects of Pol II catalytic mutants on in vivo elongation rate, processivity, gene expression, mRNA decay and response to nucleotide depletion

Indranil Malik, Chenxi Qiu, Thomas Snavely, and Craig D. Kaplan*.

*To whom correspondence should be addressed. Craig D. Kaplan, 322A Biochemistry, Department of Biochemistry and Biophysics, Texas A&M University, College Station, TX 77843, USA. E-mail: cdkaplan@tamu.edu. Phone: +1 979-845-0429

Department of Biochemistry and Biophysics, Texas A&M University, College Station, TX 77843, USA

Abstract

Genetic and biochemical studies have identified RNA polymerase II (Pol II) activity mutants that alter catalysis, which we use as tools to investigate transcription mechanisms. Gene expression consequences due to altered Pol II activity *in vivo* are complex. We find that alteration of Pol II catalysis decreases Pol II occupancy and reporter gene expression *in vivo*. Both reduced and increased activity Pol II mutants lead to apparent reduction in elongation rate *in vivo* in a commonly used chromatin IP assay, and we identify a confounding variable affecting interpretation of this assay. Pol II mutant effects on gene expression are exacerbated with increased promoter strength and gene length. mRNA degradation rates for a reporter gene are altered in Pol II mutant strains, with magnitude of half-life increases correlating both with mutants' growth and gene expression defects. Prior work has suggested that altered Pol II elongation sensitizes cells to nucleotide depletion. We reexamine this hypothesis and find that Pol II activity mutants and several elongation factor mutants respond to GTP starvation similarly to wild type and that putative elongation defects are not likely to drive the cellular response to limiting GTP.

Introduction

Gene transcription by RNA polymerase II (Pol II) is essential for all kingdoms of life and involves three distinct phases: initiation, elongation and termination. Transcription elongation proceeds through an iterative cycle of substrate selection, catalysis of phosphodiester bond formation, and enzyme translocation [Reviewed in [1, 2]]. Pausing, backtracking, and arrest of Pol II can occur during elongation. Pol II elongation factors are proposed to promote Pol II elongation by modulating these processes or otherwise enabling Pol II to overcome obstacles. Coordinated with elongating Pol II, several co-transcriptional events occur to control the fate of nascent RNAs and ensure proper gene expression [Reviewed in [3]]. Thus, it is likely that perturbation of Pol II elongation will have multi-faceted effects on co-transcriptional processes and overall gene expression. To understand the complexity of Pol II activity-mediated control of gene expression it is necessary to understand how alteration of Pol II catalytic activity relates to specific gene expression defects.

Studies from our lab and others have identified several Pol II catalytic mutants that can alter elongation rate *in vitro* [4-6]. Based on these mutants' ability to increase or decrease transcription elongation rate relative to wild type (WT), we term them "gain of function" (GOF) or "loss of function" (LOF) mutants, respectively [4]. Most of these mutants reside in a highly conserved, mobile sub-domain known as the trigger loop (TL) [4-6]. The TL is a component of the Pol II catalytic center, and can directly interact with incoming NTPs, undergoing conformational changes to promote rapid catalysis [5, 7, 8]. TL mutants have been shown to affect a number of Pol II biochemical properties including catalysis, substrate selection and transcription fidelity [5, 8]. In addition, TL mutants have been also shown to affect Pol II translocation, pausing and intrinsic cleavage properties [9-11].

The rate of transcription elongation has likely evolved to facilitate co-transcriptionality, which enhances the efficiency of pre-mRNA processing and maturation [Reviewed in [3]]. Maturation of pre-mRNA requires addition of a 7-methyl guanosine cap at the 5'-end of the transcript, splicing of introns, and addition of a poly(A) tail to the 3'-end of the transcript. Further, the pre-mRNA is uniquely packaged with protein components into a mature mRNA granule, which facilitates export and efficient translation. Impaired processing leads to degradation of pre-mRNAs by nuclear surveillance pathways. Mechanistic coupling of transcription and pre-mRNA processing is achieved through recruitment of factors by C-terminal domain (CTD) and by kinetic competition [Reviewed in [3]]. Using Pol II catalytic mutants, it has been shown that kinetic competition may govern pre-mRNA splicing and polyadenylation [12-16]. At least one Pol II catalytic mutant has been reported to be defective in 5'-capping, leading to the degradation of transcript by 5' to 3' nuclear exonuclease [17]. Additionally, a number of findings suggest kinetic competition between transcription termination and elongation in both yeast and human cells [18, 19]. Recently, a competition-independent pathway has been proposed for termination that occurs through a conformational change to Pol II [20]. Furthermore, evidence has led to proposals about connections between transcription rate and mRNA decay to maintain cellular mRNA abundance, though molecular mechanisms are unclear [21-25]. For example, growth rate is also proposed to control mRNA

decay and overall mRNA abundance, but whether mutants' effects on transcription rate or their effects on growth are the major contributing factors in alteration of mRNA decay is unknown [26-28].

In order to study Pol II elongation *in vivo*, a number of methods have been implemented that either directly measure apparent Pol II elongation rate or determine indirect consequences of elongation rate [29-32] (for a list methods and estimated *in vivo* Pol II elongation rate see here [33]). Two methods are generally used to study elongation in yeast, one to study elongation properties and the other to genetically implicate factors in elongation control. The first utilizes chromatin immunoprecipitation (ChIP) to determine Pol II occupancy across a long galactose-inducible gene, *GAL1p::YLR454w*, either in steady state or after transcription shut off by addition of glucose [29]. Apparent processivity is inferred from comparison of steady state Pol II occupancy for wild type and transcription mutants, while kinetics of the 'last wave' of Pol II leaving the template can be used to determine the apparent elongation rate (**Supplementary Table 1**). Indeed, Pol II catalytic mutants and several factors mutants have shown altered apparent *in vivo* elongation rate and apparent processivity defects in this assay. Processivity can only be inferred, because differential elongation rate over regions of the template may also explain differential occupancy. Interpretation of apparent elongation rate differences based on transcriptional shut off makes assumptions that signaling and kinetics of the shut off are identical between WT and mutant strains. Similarly, in a second widely used approach, genetic detection of elongation defects through use of nucleotide-depleting drugs makes assumptions that drug effects are identical between WT and mutant strains, and this issue is discussed below.

Nucleotide-depleting drugs, such as mycophenolic acid (MPA), which limits cellular GTP levels by inhibiting IMPDH activity, are assumed to elicit transcription elongation defects by enhancing pausing, arrest, or backtracking due to limitation in substrate levels [1, 34-37]. Growth sensitivity to MPA for Pol II or presumptive elongation factor mutants has been widely interpreted as a synergistic effect between MPA treatment and impaired elongation due to the mutant. The notion that limiting nucleotide is the major determinant of drug phenotypes was further strengthened by the observation that guanine supplementation suppresses sensitivity to the drug, along the observation of elongation defects due to drug treatment [29, 38]. However, it has been shown subsequently that many MPA-sensitive transcription mutants are defective for upregulation of MPA-resistant IMPDH activity encoded by the *IMD2* gene [39]. Under normal conditions an upstream TSS at *IMD2* is used, generating an unstable transcript that terminates within the *IMD2* promoter [40, 41]. Upon GTP starvation elicited by MPA treatment, a downstream TSS is utilized, allowing for expression of *IMD2*. Regulation of *IMD2* expression, presumably mediated by this TSS switch, is defective in a wide range of transcription elongation mutants, as well as for mutants that alter Pol II catalytic activity [4, 38, 42]. Thus, when these mutants are treated with MPA, they are exquisitely sensitive due to acute GTP starvation – starvation that WT cells do not experience when exposed to MPA, and not necessarily due to global elongation defects. Therefore, the relationship between Pol II activity and GTP starvation is muddled due to confounding variables during the induction of GTP starvation.

Here, we determined the *in vivo* consequences of a set of Pol II mutants with altered *in vitro* elongation rate. We show that altered Pol II catalytic activity affects *in vivo* Pol II occupancy and reporter gene expression. Gene expression defects correlate with gene length and promoter strength. Pol II catalytic mutants show altered mRNA decay rates and the magnitude of altered decay correlates with both mRNA expression defect and the mutants' growth defects. We observed allele-specific interaction of Pol II catalytic mutants with pre-mRNA processing factors, and found evidence that an mRNA processing defect in the catalytic mutants may lead to degradation of the transcript. Furthermore, we critically evaluated the two major widely used systems for studying transcription elongation in yeast – chromatin IP of the 'last wave' of Pol II upon transcription inhibition, and response to GTP starvation. We uncovered differential response to glucose as a confounding variable in its use to shut off transcription of a galactose-inducible elongation reporter. Given this variable, conclusions in the literature regarding *in vivo* elongation rate for a large number of transcription mutants may not be supported. Finally, we test the model that Pol II mutant defects in *IMD2* induction relate to defects in GTP sensing, and determine that Pol II or other transcription factor defects do not render GTP limiting for growth of most tested strains.

MATERIAL AND METHODS

Yeast strains, plasmid, media and growth

Yeast strains and plasmids used in this study are listed in **Supplementary Table 2 and 3, respectively**.

Yeast media are prepared following standard [43] and previously described protocols [4]. Yeast extract (1% w/v; BD), peptone (2% w/v; BD) and 2% bacto-agar (BD), supplemented with adenine (0.15mM) and tryptophan (0.4mM) (Sigma-Aldrich) comprised YP solid medium. YPD plates contained dextrose (2% w/v, VWR), YPRaf plates contained raffinose (2% w/v, Amresco), YP-Raf/Gal plates contained raffinose (2% w/v) plus galactose (1% w/v, Amresco) and YPGal plates contained galactose (2% w/v) as carbon sources. YPRaf, YPGal and YPRaf/Gal plates also contained antimycin A (1 mg/ml; Sigma-Aldrich). Minimal media plates were prepared with synthetic complete (SC) or 'Hopkins mix' with appropriate amino acid(s) dropped out as described in [43], with slight modifications as described in [4]. For studies with mycophenolic acid (MPA, Sigma-Aldrich), a stock solution (10 mg/ml, in 100% ethanol) of MPA was added to solid or liquid media to achieve desired concentration. NaOH, HCl and Guanine were added to solid media to achieve desired concentration as indicated. Liquid YPD, YPRaf, YPGal and YPRafGal media are prepared with yeast extract (1% w/v), peptone (2% w/v) and 2% (w/v) carbon source (dextrose, raffinose, galactose or raffinose plus galactose), with no supplementary adenine, tryptophan or antimycin A.

Yeast phenotyping assays were performed by serial dilution and spotting onto plates as described earlier [4]. Doubling times for the mutants in liquid medium (YPGal) were determined using Tecan plate-reader as described earlier [44], with minor modifications. Overnight grown saturated cultures were diluted to an OD_{600} of ~ 0.1 in fresh YPGal medium and grown in triplicate at 30˚C in a 96-well plate in a Tecan Infinite F200 plate reader under continuous shaking**.** Data obtained from each plate were considered as a single biological replicate and was analyzed in Graphpad Prism using an exponential-growth fitting function.

Chromatin immunoprecipitation

All the strains used for ChIP experiments contained a C-terminal epitope tag on the Rpb3 subunit of RNA Pol II (RPB3::3XFLAG::KANMX; see strain list). ChIP experiments were performed as described previously [45]. Briefly, 100 ml of mid-log phase cells (~$1x10^7$ cells/ml) were cross-linked with 1% formaldehyde (final) for 20 min, and then quenched with 15 ml of 2.5 M glycine for 5 min. Cross-linked cells were washed twice with cold 1X TBS buffer at 4˚C and were disrupted by bead beating with glass beads in lysis buffer (0.1 M Tris pH 8.0, glycerol 20%, 1 mM PMSF). Cross-linked cell lysates were subjected to a low speed spin (1500 rpm, 1 min at 4˚C) to remove cell-debris, followed by centrifugation of chromatin pellets, subsequent washing of pellets (twice) with 1 ml FA buffer (50 mM HEPES-KOH pH 7.5, 300 mM NaCl, 1 mM EDTA, 0.1% Triton X-100, 0.01% sodium deoxycholate, 0.1% SDS and 1 mM PMSF) at 14000 rpm for 20 min at 4˚C. Chromatin pellets were resuspended in 1 ml of FA buffer and sonicated at 4˚C using a Diagenode Bioruptor (45 cycles – 3 x 15 cycles; 30 sec ON/ 45 sec OFF) to generate ~300-500 bp chromatin fragments (verified on 1% agarose gel). Approximately 100 µl sonicated chromatin was used for each immunoprecipitation (IP) with anti-FLAG antibody (FLAG M2 magnetic beads, Sigma-Aldrich). Surfactant and detergent composition in buffers were changed according to manufacturer's recommendation for compatibility with M2 FLAG antibody, and all buffers contained 1 mM PMSF. For Pol II occupancy determination, the amount of chromatin used for WT or mutant IPs was normalized by starting cell number and chromatin concentration (estimated by spectrophotometer and agarose gel-lane profile). Magnetically-captured FLAG beads were washed twice with FA buffer, once with FA buffer with 500 mM NaCl, once with wash buffer (10 mM Tris-HCl pH 8.0, 0.25 M LiCl, 0.5% NP-40, 1 mM EDTA) and once with TE. Immunoprecipitated chromatin was eluted by two-step elution at 65˚C, with 100 ul and 150 ul elution buffers (50 mM Tris-HCl pH 8.0, 1 mM EDTA, 1% SDS) for 15 min and 30 min, respectively. Both eluates were pooled and incubated at 65˚C (> 6 hrs) for cross-linking reversal. 10 ul of sonicated chromatin (10% of material added to IP) plus 240 ul of elution buffer were treated identically and served as IP input control. Input or immunoprecipitated DNA was purified by standard phenol-chloroform extraction and ethanol precipitated in presence of pellet paint (MilliporeSigma) or glycoblue (ThermoFisher). Immunoprecipitated DNA and 10% of corresponding input DNA (1:10 diluted in nuclease free water) were used for qPCR with SsoAdvanced or SsoAdvanced Universal SYBR Green supermix (Bio-Rad) using CFX 96 (Bio-Rad). Fold enrichment for target amplicon over non-transcribed region was determined by the $\Delta\Delta C_T$ method [46]. Primers used for qPCR are listed in **Supplementary Table 4**.

For *in vivo* elongation assays, WT or mutant cells were grown in YPGal to mid-log phase and a pre-glucose shut off sample was taken for the 0 minute time point. Then glucose (4% final) was added to inhibit transcription and aliquots were removed after 2, 4, 6 and 8 minutes (optional longer time points were taken for some strains). Alternatively, after isolation of 0 min sample as above, remainder of culture was centrifuged and washed with SC medium lacking carbon source as described earlier [18], then inoculated in YPD (4% glucose) media or SC media lacking carbon source to isolate glucose shut off samples or galactose-depletion samples, respectively, at indicated time points. Formaldehyde cross-linking, chromatin preparation and subsequent steps were performed as described above.

RNA isolation, Northern blotting

For gene expression analysis, RNAs were isolated from mid-log phase cells grown in appropriate medium. For galactose-induction assays, cells were grown to mid-log phase in YPRaf and pre-induction sample was isolated as 0 min time point followed by addition of galactose (4% final) to the culture. Aliquots were removed as gal-induction samples at indicated time points. Likewise, for mRNA decay analysis, cells were grown to mid-log phase in YPGal and pre glucose shut off sample was collected as 0 min time point followed by the addition of glucose (4% final) to shut off transcription. Post shut off samples were collected by a quick centrifugation for 1 min and immediate freezing of the cell pellets. Centrifugation time was included while calculating shut off time. Total RNA was purified using hot phenol-chloroform method as described previously [47].

Northern blotting was performed essentially as described in the manual for GeneScreen hybridization membranes (Perkin-Elmer) with minor modifications as described earlier [4]. In brief, 20 µg of total RNA, treated with Glyoxal sample-load dye (Ambion), was separated on 1% agarose gel and transferred to membrane by capillary blotting. Pre-hybridization solution contained 50% formamide, 5X Denhardt's solution, 10% Dextran sulfate, 1 M NaCl, 50 mM Tris-HCl pH 7.5, 0.1% sodium pyrophosphate, 0.1% SDS and 500 µg/ml denatured salmon sperm DNA. PCR generated DNA double-stranded probes for northern blots were radiolabeled with ^{32}P-dATP using the Decaprime II kit (Ambion) according to manufacturer's instructions. After overnight hybridization of the blot at 42˚C, washes were done twice each in 2X SSC for 15 minutes at 42˚C, in 5X SSC with 0.5% SDS for 30 minutes at 65˚C, and in 0.2X SSC for 30 minutes at room temperature. Blots were visualized by phosphorimaging (Bio-Rad or GE Healthcare) and quantified using Quantity One (Bio-Rad).

Northern blotting for mapping the termination window of the pre-processed snR33 transcript was performed essentially as described in [18, 48] with minor modifications. Briefly, 5-8 µg of RNA were separated on 6% polyacrylamide-7M urea gel. RNAs were transferred from polyacrylamide gel to a membrane (GeneScreen Plus, PerkinElmer) with a Bio-Rad Trans-Blot apparatus at a setting of 45W for 1.5 hrs. RNAs were cross-linked to the membrane by UV light. Pre-hybridization of the membrane, probe synthesis and membranes-hybridization were performed as described in [48]. Membranes were washed twice with low stringency wash buffer (0.1x SSC, 0.1% SDS) and visualized by phosphorimaging (Bio-Rad or GE Healthcare). Lane traces were determined for each sample using ImageQuant (GE Healthcare).

Primer extension

For primer extension (PE) analysis, RNA was isolated from mid-log phase cells grown in appropriate media, optionally treated with desired concentration of MPA for indicated time periods. Primer extension analysis was done essentially as described earlier [49] with modification described in [4]. Briefly, 30 µg of total RNA was annealed with ^{32}P end-labeled oligo. M-MLV Reverse Transcriptase (Fermentas) was used for reverse transcription, in the presence of RNase Inhibitor (Fermentas). Primer extension products were ethanol precipitated overnight and separated on 8% polyacrylamide gels (19:1 acrylamide:bisacrylamide, Bio-Rad) containing 1X TBE and 7M urea. PE gels were visualized by phosphorimaging (Bio-Rad or GE Healthcare) and quantified using Image Lab software (Bio-Rad).

Microscopy and image analysis

Mig1p-GFP tagged strain was made by integrating GFP C-terminal tag at the genomic locus (see strain description). Microscopy was performed as described previously [50], with modifications. Briefly, cells grown overnight in SC medium (2% galactose) at 30˚C, diluted in fresh SC media and grown till mid-log at 30˚C before microscopy. Perfusion chamber gasket (ThermoFisher, 4 chamber: 19 mm X 6 mm) was

used for changing medium. Chamber was treated with Con A (2 mg/ml, MP Biomedicals) for 10-15 min, and then cells were injected into the chamber and allowed 10-15 min to adhere. Medium exchange from SC (2% galactose) to SC (2% galactose) + glucose (4% final) was done by pipetting quickly, while the chamber is fixed on the microscope stage. Pre-glucose sample was considered as time 0 and glucose repression time points were taken immediately after exchange of the medium.

For Mig1p-GFP nuclear localization kinetics, microscopy was performed with an inverted epifluorescence microscope (Ti-E, Nikon, Tokyo, Japan) using a 100x objective (Plan Fluo, NA 1.40, oil immersion) and standard filter sets. Images were acquired using a cooled EMCCD camera (iXon3 897, Andor, Belfast, United Kingdom). For delayed Mig1p response (longer time points), microscopy was performed with a Nikon Ti-E microscope equipped with a CFI Plan Apo lambda DM 100x objective and a Prior Scientific Lumen 200 Illumination system. All images were acquired using NIS Element software and data analysis was done using Quantity One (Bio-Rad). Ratio of nuclear/cytoplasmic GFP intensity was calculated as [(nuclear GFP intensity – background) / (cytoplasmic GFP intensity – background)]. Obtained values for glucose repression time points were normalized to pre-glucose (time 0, t0) value. Non-responding cells were quantified similarly, except for the fact that there was no visible nuclear foci, thus a random, central area was selected and measured for fluorescence intensity. Position and area of the measurement was kept identical for all the time points for the same cell. We reasoned that a non-responding cell would not have a distinct change over time in nuclear/cytoplasmic GFP intensity, hence quantifying a random area as nucleus should not have an overall affect on the interpretation of the data.

RESULTS

Pol II catalytic mutants alter steady state Pol II occupancy and apparent processivity.

Previously we reported genetic and biochemical dissection of Pol II catalytic mutants as probes for transcription mechanisms [4, 5, 51]. To explore *in vivo* consequences of altered Pol II activity, we examined Pol II occupancy by chromatin IP for a subset of LOF and GOF Pol II mutants over a widely used inducible long reporter gene, *GAL1p*::*YLR454w* (**Figure 1A** and [29]). We observed decreased overall polymerase occupancy for GOF and LOF mutants compared to WT (**Figure 1B**). Among the mutants tested, H1085Y (strong LOF) and G1097D (strong GOF) showed the most severe defects in Pol II occupancy, consistent with their severe growth defects *in vivo* [4]. A number of polymerase and transcription associated factor mutants confer reduced Pol II occupancy over the 3' end of *GAL1p*::*YLR454w*, and this defect has been previously interpreted as a defect in Pol II processivity [29]. When we normalized the Pol II fold-enrichment over the 5' end of the gene body ("1kb" amplicon) followed by normalization of mutant values to WT, catalytic mutants show selective decrease in occupancy over the 3' end of the reporter (most obvious for G1097D) (**Figure 1C**). While decreased Pol II occupancy is consistent with a gradient of Pol II dissociation or degradation across a transcription unit, it is also consistent with alterations in Pol II elongation rate over gene bodies as have been observed in mammalian cells [52-54]. ChIP is unable to distinguish between the two possibilities.

Additional factors may determine Pol II occupancy levels over genes. For example, Pol II occupancy over a template can be gene class-dependent or regulon-specific, and external perturbations such as changes in temperature or carbon source can affect transcription [55, 56]. Here we examined Pol II occupancy over the same reporter driven by a constitutive promoter (*TEF1p*::*YLR454w*) for the most severely defective Pol II LOF and GOF mutants grown in glucose- or galactose-containing medium (**Figure 1D and E**). In contrast to *GAL1p*::*YLR454w* occupancy, here we observed a increased Pol II occupancy for H1085Y in galactose relative to glucose, with the converse for G1097D, compared to WT (**Figure1E**), although, a 3' occupancy defect was still apparent for both mutants. Further, G1097D 3' occupancy defect appeared to be less severe in galactose compared to glucose, suggesting this particular mutant or, this class of mutants may behave differently in glucose and galactose. WT Pol II showed more subtle changes in occupancy in glucose relative to galactose.

Pol II catalytic mutants alter reporter gene expression with exacerbating effect of increasing gene length and promoter strength.

Decreased Pol II occupancy for some mutants could be explained by increased elongation rate, leading to reduced steady state levels of Pol II on genes. Alternatively, defective initiation or elongation might

lead to decreased Pol II occupancy [57]. Pol II activity mutants do perturb initiation as most or all show defects in TSS selection [14, 51]. Mutants affecting Pol II elongation also have been shown to affect reporter gene expression depending on nature of transcription unit driven by identical promoters, allowing presumptive elongation defects to be distinguished from initiation defects, using the so-called GLAM assay [32, 58]. To determine how Pol II catalytic mutants affect gene expression, and expression defects relate to gene length and/or promoter strength, we measured effects on expression of *YLR454w* (in different promoter contexts), endogenous *TEF1*, and endogenous *GAL1* by northern blotting (**Figure 2A and B**). We observed strong effects on *GAL1-YLR454w* expression in Pol II mutants compared to WT, with the magnitudes of effects higher than for defects in occupancy, especially for H1085Y and G1097D. Although the expression defect in H1085Y can be explained by slow elongation based on its *in vitro* elongation rate, results for G1097D and E1103G, predicted to be fast for elongation, suggest they have occupancy defects for reasons other than merely being fast *in vivo*.

Furthermore, we determined that Pol II catalytic mutants show greater gene expression defects for *GAL1-YLR454w* than for the more lowly expressed *TEF1-YLR454w*. We also examined native *TEF1* and *GAL1* expression levels in Pol II mutants and found greater expression defects for the longer *YLR454w* transcription unit versus the native transcription units, and for more highly expressed promoters relative to promoters generating lower expression levels. These results are consistent with previous observations showing Pol II occupancy and gene length dependent effects of reporter expression for several elongation mutants [32, 58]. Given reduced Pol II occupancy and gene expression, it is likely that initiation defects might also be in play, especially due to the fact that all Pol II catalytic mutants tested here show defects in TSS selection [14, 51]. Examination of the activation kinetics for *GAL1p*::*YLR454w* or *GAL1* revealed delayed induction for Pol II catalytic mutants, consistent with defects in activation or initiation (**Figure 2C**).

Pol II catalytic mutants show allele-specific genetic interactions with pre-mRNA processing factors.

Eukaryotic mRNA processing includes the addition of a 5' cap and a 3'-poly(A) tail that protects mRNA from degradation by 5' exonucleases and 3' exonucleases, respectively. While mRNA degradation predominantly occurs in cytoplasm, dedicated exonucleases are present in the nucleus for surveillance and degradation of defective, improperly packaged, or prematurely terminated RNAs. We reasoned that an mRNA processing defect or premature termination could lead to degradation of pre-mRNA by 5' or 3'-exonucleases, respectively, resulting in decreased abundance of *GAL1-YLR454w*. We first determined if Pol II mutants showed genetic interactions with known exonucleases that function in surveillance. Deletion of Rrp6, a component of the 3'-exonuclease exosome complex, showed a slight negative genetic interaction with Pol II GOF mutants (**Figure 3A)**. Inactivation of Rat1 and Xrn1, two 5'-exonucleases, showed strong genetic interactions with GOF mutants (**Figure 3A**). Rat1 is essential and functions in termination of Pol II at protein-coding genes [59, 60]. LOF mutants partially suppressed the Ts$^-$ phenotype of *rat1-1*, a conditionally viable allele of *RAT1*. In contrast, GOF Pol II alleles showed synthetic sick interactions with *rat1-1*, consistent with prior findings and model proposed for kinetic competition between termination and elongation [18, 19, 61]. Rat1 works with an activating partner Rai1, which processes partially capped mRNA allowing Rat1 access [62]. Growth defect of *rai1*Δ was slightly suppressed by both LOF and GOF mutants at 37˚C, while *dxo1*Δ, a recently described nuclear 5'-exonuclase [63], showed no strong genetic interactions with Pol II alleles (**Figure 3A**).

We then asked if mRNA processing mutants that show genetic interactions with Pol II mutants were able to modulate Pol II alleles' gene expression defects. As expected, deletion of Rrp6 did not recuse full-length *GAL1*p::*YLR454w* expression level significantly; the nuclear exosome would be expected to mainly degrade prematurely-terminated transcripts (**Supplementary Figure 1A**). Deletion of Xrn1 slightly rescued *GAL1*p::*YLR454w* expression level in E1103G, while inactivation of Rat1 severely decreased *GAL1*p::*YLR454w* expression level in both WT and catalytic mutants possibly due its growth defect (**Supplementary Figure 1A and B)**. We found that *xrn1*Δ/*rat1-1* double mutant strains were extremely sick on YPGal even at permissive temperature (**Supplementary Figure 1C**). Hence, for determination of *GAL1*p::*YLR454w* expression level we used YPRaf/Gal liquid medium lacking Antimycin A, which allows growth of Pol II mutants in the *xrn1*Δ/*rat1-1* background. Ordinarily, YPGal liquid is generally used to determine *GAL1*p::*YLR454w* expression. We observed appearance of an internal cryptic *GAL1*p::*YLR454w* transcript in *xrn1*Δ/*rat1-1* mutant background, as reported earlier for an

spt16 mutant [**Figure 3B** and [64]]. Intriguingly, inactivation of both Xrn1 and Rat1 together completely rescued the *GAL1*p::*YLR454w* expression level in E1103G (*xrn1*Δ/*rat1-1*) compared to WT (*xrn1*Δ/*rat1-1*) at 37˚C (**Figure 3B**), suggesting possible processing-defective transcripts in E1103G are stabilized by inactivation of Xrn1 and Rat1.

Altered mRNA half-life of the reporter correlates with gene expression and growth defects in Pol II catalytic mutants.

The abundance of cellular mRNAs is determined by synthesis and degradation rates. In order to determine if the Pol II mutants altered half-life of the *GAL1*p::*YLR454w* mRNA, we performed transcriptional shut off by addition of glucose followed by measurement of mRNA over time by northern blotting. mRNA half-lives were determined by fitting decay curves with a lag followed by exponential decay (**Supplementary Figure 2A**). The observed lags comprise the cellular response time for transcriptional shut off, the time for engaged Pol II to run off the gene, and the time for mRNA to be exported from the nucleus as the major mRNA decay pathways are cytoplasmic. Such lags have been observed in genome-wide experiments that block initiation and allow elongation to proceed [65]. We found that all GOF and LOF mutants conferred an increase in the half-life of *YLR454w*, in addition to showing longer lag periods compared to WT (**Figure 4A, Supplementary Figure 2B-H**). These results suggest a number of conclusions. First, they indicate defects in mRNA synthesis rates for all tested Pol II mutants, as expression is reduced relative to wild type even though the *GAL1-YLR454w* mRNA was more stable. Second, longer lag periods may indicate delayed response for transcriptional shut off, slower elongation rate on this template, or delayed mRNA export for these mutants (addressed below). These observations indicate that mutant effects on mRNA degradation may be difficult to deconvolute from their effects on growth, given that growth rate also a factor in mRNA decay rates. Indeed, we observed that mRNA half-lives inversely correlated with reporter gene expression while positively correlating with strain doubling times (**Figure 4B and 4C, Supplementary Figure 2I-J**).

Pol II catalytic mutants exhibit slower apparent *in vivo* elongation rate on *GAL1*p::*YLR454w* template in a glucose shut off assay.

In our mRNA decay experiments, longer lag times prior to exponential decay for LOF mutants are consistent with predicted elongation defects and delayed clearance of the template. Conversely, GOF mutants are predicted to run off the template more quickly. In contrast, GOF mutants also showed longer lags prior to exponential decay. These lags could be consistent with reduced kinetics for one of the following – glucose sensing, Pol II running off the template, or mRNA export. One GOF mutant tested here, E1103G, was previously suggested to be faster than WT *in vivo* based on chromatin IP analysis of the same *GAL1*p::*YLR454w* reporter [18]. To examine this further, we employed the widely used glucose shut off of *GAL1*p::*YLR454w* to measure the last wave of Pol II transcription (**Figure 5A**) [29]. As predicted, LOF mutants N479S and H1085Y showed extensive delay compared to WT in Pol II run-off kinetics subsequent to transcriptional shutoff by the addition of glucose to the medium (**Figure 5B and D**). The apparent *in vivo* elongation rate of H1085Y was slower than N479S, which is consistent with its stronger growth defects and *in vivo* phenotypes relative to N479S. This is in slight contrast to previous *in vitro* measurements indicating N479S Pol II as slower than H1085Y. However, in direct contrast to previous observations and predictions, both the GOF mutants tested here, E1103G and G1097D, also showed reduced kinetics of Pol II runoff subsequent to glucose shut off (**Figure 5C**). This result was unexpected, especially when E1103G seemed to have faster elongation rate than WT in this assay [18]. Furthermore, analogous substitution in human POLR2A E1126G confers a slightly faster than WT elongation rate *in vivo* [12]. It is important to note that there are distinctions between glucose shut off protocols used by us and by Hazelbaker et al [18]. In order to understand the nature of the observed discrepancy, we first confirmed our GOF mutant strains by three steps – i. confirmation of the mutation by sequencing, ii. transcriptional growth phenotypes as described in [4], and iii. mutants ability to shift transcriptional start sites (TSSs) at the *ADH1* promoter as described in [4, 14, 51] (**Supplementary Figure 3A**). In all cases, results were consistent with correct strains showing expected phenotypes. In addition, we analyzed the *SNR33* termination window in these mutants. It has been proposed that kinetic competition between elongating Pol II and Sen1 helicase determines the termination of the snR33 transcript [18]. Deletion of the nuclear exosome subunit Rrp6 stabilizes pre-processed snR33 intermediate transcripts allowing detection of the snR33 termination window by examination of snR33 transcript length (**Figure 6A**). Both GOF mutants E1103G and G1097D increase the average length of

pre-processed snR33, which is in agreement with previous observations for E1103G (**Figure 6B** and [18]). Conversely, LOF mutants N479S and H1085Y decreased the average length of pre-processed snR33 (**Figure 6B**). Average length of pre-processed snR33 is longer in G1097D than E1103G, consistent with faster *in vitro* elongation rate of G1097D than E1103G, and is shorter in H1085Y than N479S, consistent with slower apparent *in vivo* elongation rate shown in this study (**Figure 5D**). We also observed alternative mature snR33 transcripts longer or shorter in length for GOF and LOF mutants, respectively, consistent with increased upstream or downstream utilization of transcription start site (TSS) in these mutants.

Next, we measured the *in vivo* elongation rate for E1103G using the protocol as described in Hazelbaker et al [18], with one important addition. The prior study utilized a no sugar wash between growth in galactose and resuspension of cells in glucose-containing medium. Our addition was to take a time point just post wash (W0) to determine if this wash step was neutral in regards to Pol II occupancy, in addition to the pre-wash "zero" used by Hazelbaker et al [18]. In our hands, E1103G was slower exiting the template than WT, consistent with our direct glucose shut off without washing, and our measurement of increased lag prior to exponential RNA decay following shutoff of this mutant (**Figure 5E**). Furthermore, Pol II occupancy at the W0 time point shows evidence of transcriptional shutoff due to absence of sugar during the wash, indicating that any variability in duration of this step would have effects on determination of presumptive elongation rates. We confirmed the observed decrease in Pol II occupancy is not due to delayed formaldehyde cross-linking, as we did not observe any difference in Pol II occupancy when crosslinking was simultaneous with the addition of glucose (**Supplementary Figure 3B**). E1103G Pol II exhibits a loss of occupancy over the 3'-end of *GAL1*p*::YLR454w* compared to WT following the no sugar wash that was not observed when transcription was shut off with addition of glucose (**Figure 5C and 5E**). In order to examine this further, we performed a galactose starvation time course where no sugar was added. This experiment showed similar 3' specific runoff in E1103G early in the time course, and not seen under glucose shutoff (**Figure 5F**). As polymerases (presumptively) run into the gene 3' end at later time points, the effect diminishes. Additionally, in this iteration of the experiment there appears to be faster loss of E1103G from the 5' end of the reporter early, though E1103G is maintained much longer later in the time course (**Figure 5F**).

Glucose repression signaling involving Mig1 nuclear translocation is aberrant in Pol II GOF mutants

One possibility for apparent slower elongation of GOF mutants on the *GAL1*p*::YLR454w* template could be delayed transcriptional shut off. We reasoned that if glucose-repression were delayed in GOF mutants, it would contribute to apparent slow kinetics of Pol II exiting the gene. To this end, we investigated the kinetics of nuclear localization of Mig1p, which upon addition of glucose to medium is imported into the nucleus due to regulation by dephosphorylation, binds to target promoters of glucose-repressed genes and recruits co-repressors [66, 67]. As a proxy for early events in this cascade, we determined the kinetics of Mig1p nuclear localization by monitoring import of Mig1p-GFP upon glucose addition in WT or GOF catalytic mutants [50]. We observed the concentration of Mig1p fluorescence signal (presumably localizing to the nucleus) saturate within ~2 min for WT cells, as previously reported [68]. However, the GOF mutants did not appear to reach maximum nuclear fluorescence within 2 min of glucose addition, thus we measured extended time points and analyzed the data using non-linear regression (**Figure 7A and B**). G1097D showed both a delay in average time of Mig1p nuclear import and reduced average maximum nuclear fluorescence compared to WT, suggesting at least in this mutant *in vivo* shut off kinetics may be delayed due to deranged Mig1p signaling (**Figure 7B**). When we measured extended time points, a noticeable subset of delayed responding cells was observed again for G1097D, while higher fractions of non-responding cells were observed for both E1103G and G1097D.(**Figure 7C** and **Supplementary Figure 4**). Altogether these results indicate that aberrant Mig1 nuclear translocation can be one of the attributing factors for apparent slower elongation observed for GOF mutants.

Pol II catalytic mutants and transcription factor mutants do not generally alter sensitivity to the GTP-depleting drug MPA in the absence of *IMD2*

Nucleotide depleting drugs such as MPA or 6-AU have been interpreted in the past as specifically exacerbating elongation defective Pol II or transcription factor mutants. Such interpretations of MPA

treatment are complicated by differential nucleotide starvation of WT and factor mutant strains due to differences in gene expression of *IMD2*, whose gene product is required for resistance to MPA [69-71]. To evaluate how Pol II responds to GTP starvation and determine whether Pol II transcription is a critical determinant for cellular sensitivity to GTP starvation, we employed a strategy to normalize GTP starvation upon MPA treatment across strains by deletion of *IMD2* (**Figure 8**). To enable an *in vivo* readout for *IMD2* expression, we replaced the *IMD2* ORF with *HIS3* (**Figure 8A**).

In the absence of *IMD2*, yeast strains become hypersensitive to MPA treatment as expected (**Figure 8B**) [69, 70]. If Pol II transcription were a major determinant of GTP starvation, relative to all other cellular GTP-dependent processes, it would be predicted that elongation-defective Pol II alleles would be additionally hypersensitive to MPA, while increased catalytic activity mutants would be resistant. In contrast to these predictions, deletion of *IMD2* strongly blunts the Pol II allele-specific effects of MPA treatment on yeast cells (**Figure 8B**). We do in fact observe very mild MPA sensitivity for Pol II GOF alleles, but these effects are counter to expectations of the widely presented model for Pol II response to GTP starvation. These results suggest that the major determinant for Pol II allele sensitivity to MPA is differential *IMD2* expression, and that Pol II transcription is not a major determinant for sensitivity to GTP starvation in the absence of *IMD2*. MPA effects are presumed to function through GTP starvation as indicated by suppression of sensitivity upon addition of guanine to the growth medium, allowing an alternate route for GTP synthesis. In testing this presumption, we found that addition of 10 mM NaOH to medium on its own abrogated any MPA effects, likely through alteration of MPA solubility (**Supplemental Figure 5**). Furthermore, Pol II mutants show allele-specific phenotypes upon change to pH of media [10]. As basic conditions are required for guanine solubility in stock solutions, this confounds previous interpretations where pH effects of guanine addition, or on mutant phenotypes, were not controlled. We determined that addition of guanine/NaOH or NaOH alone to medium, followed by neutralization of NaOH with equivalent HCl, with subsequent MPA addition allowed for both MPA and guanine to coexist in media (**Figure 8B**). We observed almost but not complete suppression of MPA by addition of guanine, with mild sensitivity of GOF mutants to MPA in the presence of guanine. These results suggest that either the *IMD2*-independent MPA effects on GOF mutants are independent of GTP starvation, or these mutants have alterations in their GTP salvage synthesis pathways.

We next determined if the ability to induce the *IMD2* promoter was maintained in Pol II mutants when GTP starvation conditions were normalized, using growth on medium lacking histidine to detect expression of *imd2Δ::HIS3* (**Figure 8C**). WT cells were almost completely His^- in the absence of induction of the *IMD2* promoter (controlling *HIS3*), while LOF mutants were His^+, indicative of constitutive expression of *imd2Δ::HIS3*. All strains showed induction of His^+ phenotype upon induction of the *IMD2* promoter suggesting that productive transcription from the *IMD2* promoter was possible for all tested Pol II mutants (discussed further below).

A number of transcription factor mutants have been described as either MPA or 6-AU sensitive with these sensitivities interpreted as indicative of Pol II elongation defects. Such mutants include deletions in known elongation factor genes *dst1*Δ (encodes TFIIS, [42, 72]), *spt4*Δ (subunit of Spt4/Spt5 DSIF, [73-75]), *paf1*Δ (Paf1C complex member, [38, 76]), *bur2*Δ (P-TEFb subunit homolog, [74]), *pop2*Δ (encodes Ccr4/NOT complex member, [42, 77]) or deletions in genes encoding subunits of transcriptional coactivator complexes *spt3*Δ, *sgf73*Δ (SAGA, [38, 42]) or *gal11*Δ (Mediator, [42]). It has previously been demonstrated for some of these mutants that *IMD2* induction is defective [38, 42], indicating differential GTP starvation upon drug treatment for these strains relative to WT, just as for Pol II mutants. As above, we characterized these strains' sensitivity to MPA treatment in the absence of *IMD2* (**Figure 9**). We observed a wide range of behaviors for these strains in presence or absence of *IMD2* (**Figure 9A**). First, not all were sensitive to MPA. Second, only *spt3*Δ maintained MPA hypersensitivity in the absence of *IMD2* relative to WT, while *dst1*Δ showed only slight sensitivity relative to WT. We next examined suppression of observed MPA sensitivities by guanine supplementation (Figure 9A, bottom panels). We observed that *spt3*Δ was entirely suppressed by guanine, *dst1*Δ mostly suppressed, and *spt4*Δ, *paf1*Δ, and *gal11*Δ much less so. We hypothesize that *spt3*Δ hypersensitivity relates to defects in *TPO1* expression, as shown previously. *TPO1* encodes a transporter known to modulate MPA sensitivity [38]. Conversely, other factors can show sensitivity to MPA even in the presence of guanine. Taken together, these results are inconsistent with putative global Pol II transcription defects being a critical determinant for cell growth under GTP limitation.

We further examined if *IMD2* promoter function in response to MPA were intact in the cohort of transcription factor mutants tested (**Figure 9B**). We observed a His^+ phenotype consistent with constitutive expression of *imd2*Δ*::HIS3* in *spt4*Δ. This phenotype suggests possible altered initiation in *spt4* mutants as observed in LOF Pol II mutants (**Figure 8C**). Furthermore, we observed that the His^+ phenotype was inducible for all factor mutants except *spt3*Δ in the presence of MPA. These results indicate that presumptive GTP sensing is maintained in most mutants but that *spt3*Δ cells have a distinct defect not observed for other factor mutants or Pol II mutants. This defect indicates an almost complete inability to induce the *IMD2* promoter::*HIS3* reporter, although *spt3*Δ expresses *IMD2* upon MPA treatment at a very low level in presence of endogenous *IMD2* [42].

Pol II catalytic mutants do not abolish the response to GTP depletion but derange TSS usage at *IMD2* promoter.

By removing the possibility of differential *IMD2* expression complicating the MPA response (using *imd2*Δ), we showed above that many factor mutants or Pol II catalytic mutants have similar responses to MPA treatment. These results indicated Pol II transcription is not especially sensitive to presumptive GTP starvation *in vivo* relative to other pathways that rely on GTP (**Figure 8 and 9**). To better understand the mechanism of *IMD2* expression defects in the absence of differential GTP starvation, we further analyzed transcriptional responses at the *IMD2* promoter upon MPA treatment. Using the same *imd2*Δ::*HIS3* reporter construct used above, we analyzed the kinetics of TSS utilization upon addition of a concentration of MPA that induces a TSS shift at the *IMD2* promoter (**Figure 10A**). Pol II has been proposed to directly sense GTP levels through its active site, and through this sensing Pol II catalytic activity controls *IMD2* TSS usage [41]. Under this model, it would be predicted that LOF Pol II mutants might show precocious downstream TSS usage; indeed, this behavior has previously been observed [4]. Conversely, catalytically GOF Pol II mutants would show delayed TSS shifting kinetics due to their relative insensitivity to reduced GTP levels.

We observed that both LOF (H1085Y) and GOF (E1103G) mutants gradually lose upstream 'G' sites (**Figure 10B**), indicating retention of ability to respond to GTP-depletion. As expected WT cells rapidly lose upstream 'G' TSSs and subsequently gain the downstream functional 'A' TSS (**Figure 10C**). H1085Y constitutively uses the downstream functional 'A' TSS and shows increased usage of this site upon GTP depletion, while still showing decreased kinetics of loss of upstream TSSs. This result is unexpected from the "defective GTP sensing" model (**Fig 10 B and C**). E1103G shows reduced kinetics of loss of upstream site, consistent with defective GTP sensing, but shifts TSS usage to novel TSSs predicted to be nonfunctional due to their position upstream of the *IMD2* Nab3/Nrd1-dependent terminator (**Figure 10B and C**). If terminated by the Nab/Nrd pathway, putative non-functional novel TSSs should produce CUTs that are degraded by the nuclear exosome [78, 79]. Indeed, deletion of exosome subunit Rrp6 stabilized these transcripts derived from these novel TSSs, with significant utilization of these TSSs in E1103G compared to WT (**Figure 10D** and **Supplementary Figure 6A-B**). As expected these non-functional CUTs did not provide MPA resistance in sensitive GOF mutants (**Supplementary Figure 6C**). We note that although E1103G generally appears unable to utilize downstream functional 'A' TSS upon MPA treatment, enough functional transcript is made to produce the observed His^+ phenotype at low concentrations of MPA treatment (**Figure 9B**).

Discussion

Examination of Pol II catalytic mutants by our lab and others has shown Pol II activity-sensitive aspects of transcription initiation, elongation, co-transcriptional processes, and termination [4, 12, 14, 18, 19, 51]. In order to understand Pol II mechanisms and utilize Pol II mutants to probe co-transcriptional processes, we require interrogation of hypotheses about elongation *in vivo*. Our current study utilizes a set of yeast Pol II catalytic mutants to probe broad aspects of gene expression *in vivo*. Importantly, we investigated two widely used transcriptional reporter assays and revealed critical limitations to each assay, suggesting caution in their use and interpretation going forward.

We show that Pol II catalytic defects lead to a decrease in overall Pol II occupancy with reduction in 3' end occupancy on a galactose inducible reporter gene, *GAL1*p::*YLR454w* (**Figure 1**). Further, using a constitutively expressed *TEF1*p::*YLR454w* reporter we find that growth on different carbon sources alters occupancy profiles for both WT Pol II and catalytic mutants (**Figure 1**). Previously, several observations suggested alteration of Pol II activity and gene expression due to external perturbations such as carbon source or temperature [55, 56]. Likewise, environmental stress has also been shown to affect Pol II activity and gene expression [80]. Notably, it has also been shown that RAS/PKA signaling pathway, which controls aspects of glucose signaling, can target proteins associated with general transcription machinery, can putatively regulate elongating Pol II by targeting Spt5/4 [81, 82], and shows interactions with Nab3/Nrd1 termination factors [83]. In addition to differential effects of carbon source on steady state Pol II occupancy, we observed a differential 3'-end effect for the GOF mutant E1103G when transcription was shut off by galactose starvation relative to shut off by addition of glucose (**Figure 5**). Further, our data indicate that at least one tested GOF mutant, G1097D, is impaired in glucose repression kinetics (**Figure 7**). Taken together these results indicate growth condition-dependent modulation Pol II elongation *in vivo*. Galactose induction of *GAL* genes is also defective in both LOF and GOF mutants, with both classes showing impaired growth at 37˚C on galactose (**Supplementary Figure 1B**). It is likely that temperature further exacerbates the already large defects in Pol II mutants seen for highly expressed *GAL* genes and galactose-inducible reporters. Such defects likely arise from the sum of a number of distinct individual defects in initiation, elongation, and termination.

Pol II E1103G, which was reported previously to be fast for elongation *in vivo* relative to WT, appears slower than WT in our study. We have identified a possible artifact of prior experimental design that may have contributed to discrepant results reported here from those reported elsewhere. First, we have shown that galactose starvation, which will occur during washing of cells as described in Hazelbaker et al, shows relatively fast kinetics of transcriptional shut off at *GAL1*p::*YLR454w* [18]. Second, *GAL* promoter shut off by galactose starvation shows at least two differences in Pol II behavior compared to inhibition by glucose. During galactose starvation, E1103G Pol II runs off both the 5' and 3' ends of the reporter faster than WT (**Figure 5F**). 5' runoff is consistent with E1103G elongating faster than WT early in the time course, or E1103G being more sensitive to galactose starvation. Increased runoff kinetics from the 3' end of the reporter in E1103G is perplexing. This observation suggests that Pol II could be differentially affected while on the 3' end of the gene relative to the middle under different growth conditions. If elongation properties are expected to be uniform across a transcription unit, loss of Pol II occupancy should occur in a polar fashion from 5' to 3', as is observed under glucose shut off conditions for WT Pol II. Furthermore, after these early effects observed for E1103G relative to WT under galactose starvation, E1103G Pol II shows a delay clearing the template at longer time points regardless of mechanism of shutoff, just as purported LOF Pol II alleles do under glucose inhibition.

In vitro biochemical studies, including direct observations of individual polymerases at the single molecule level, have repeatedly shown faster elongation rate for E1103G compared to WT [4, 6, 9, 11]. Several lines of evidence suggest E1103G *in vitro* GOF activity manifests itself *in vivo* through transcriptional effects distinct from LOF mutants. First, primer extension analysis shows that E1103G shifts TSS usage upstream at a number of promoters, consistent with a model that increase in catalytic activity increases initiation probability during Pol II promoter scanning, resulting in observed upstream TSS shifts [4, 14]. Second, E1103G and other Pol II GOF mutants show allele-specific genetic interactions with a number of factors, suggesting their defects are distinct from LOF mutants [14]. For example, the synthetic sick genetic interaction of E1103G with the RNA processing factor alleles *rat1-1* and *xrn1*Δ/*rat1-1*, which are suppressed by LOF Pol II alleles, are consistent with exacerbation of termination defects through faster elongation [17-19, 61].

Delayed termination for E1103G was observed in Hazelbaker et al [18] through observation of increased length of pre-processed snR33, which we reproduce (**Figure 6**). We further show that an even stronger GOF mutant, G1097D, shows a corresponding increase in pre-processed snR33 length relative to E1103G or WT. While these results are consistent with increased elongation rate, they are also consistent with possible defective termination. As Pol II conformational changes, including those that may occur with participation of the trigger loop, have been implicated in termination mechanisms, altered termination probability should not be ruled out as possible mechanism [20]. Previous observations that

addition of 6-AU or shifting cells to higher temperature, which lead to apparent decreases or increases in elongation rate, respectively, also decrease or increase pre-processed snR33 length, extended the correlation between this assay and predicted elongation rate changes [18]. Finally, a recent study demonstrated that an E1103G strain displays a shift in cotranscriptional splicing towards downstream positions, consistent with Pol II traveling further prior to splicing (alternatively, splicing could be delayed) [15]. Altogether, these data are consistent with increased elongation kinetics in GOF catalytic mutants *in vivo* under a parsimonious view. We identify slow Mig1p nuclear translocation upon glucose exposure as a possible explanation for delayed kinetics of Pol II clearance of *GAL1*p::*YLR454w* for the severe GOF allele G1097D. There may be additional untested steps in inhibition specific to the *GAL* system that are defective, or defects specific to the long *YLR454w* template for Pol II GOF strains. Regardless, careful consideration of possible variables in assay behavior is urged given the results we present.

In order to exploit the existing transcription reporter systems to probe transcription mechanism carefully we need a detailed understanding of each phenotypic system, such as our analyses to dissect the Spt$^-$ phenotype of Pol II GOF alleles [84]. Here we investigated Pol II catalytic mutants and several transcription factors mutants' response to nucleotide-depleting drug MPA under conditions where differential *IMD2* expression was obviated. Most tested Pol II mutants and many transcription factor mutants behave similarly to WT upon MPA treatment of *imd2*Δ strains (**Figure 8 and 9**). Our results also suggest *IMD2*-independent mechanisms of MPA sensitivity, which have been observed in previous studies including large scale deletion screens for MPA or 6-AU sensitivity, have identified Pol II mutants and transcription factor mutants that do not affect *IMD2* transcription and likely to be sensitive in *IMD2*-independent ways [38, 42]. Our previous analyses identified a correlation between MPA sensitivity of Pol II GOF alleles and upstream shifts in TSS usage at *ADH1* [4, 14]. As *IMD2* regulation proceeds by initiation shifting from an upstream non-productive TSS to a downstream productive one, it is conceivable that initiation defects underlie Pol II mutant MPA sensitivity. Given differential presumed GTP starvation of Pol II GOF mutant strains when *IMD2* is present, it was difficult to determine why Pol II GOF strains were MPA sensitive. An attractive model is based on the differential sensitivity to reduced GTP levels between GOF and WT Pol II. Increased catalytic efficiency of GOF alleles might be expected to buffer GOF Pol II from reduction in GTP levels, delaying the switch from *IMD2* upstream GTP-initiated TSSs to downstream ATP-initiated TSSs, increasing acute GTP starvation possibly beyond a critical threshold for growth/viability. Here we present evidence that MPA sensitivity of the Pol II GOF allele E1103G correlates with usage of novel TSSs that are intermediately positioned between the known productive -106 A TSS at *IMD2* and upstream non-functional starts. We conclude that *IMD2* defects in Pol II GOF E1103G are likely to derive from initiation defects (**Figure 10**).

Our Pol II catalytic mutants and pre-mRNA processing factor genetic interaction data show allele-specific genetic interactions (**Figure 3**), as noted above. Synthetic sick interaction of GOF with *xrn1*Δ and stabilization of *GAL1*p::*YLR454w* transcript in *xrn1*Δ/*rat1-1* double mutant background is suggestive of a 5'-end processing defect in GOF mutants, possibly a capping defect. A defect in capping would be predicted to expose mRNA to the action of 5' exonucleases Xrn1 and Rat1. Capping of nascent transcripts occurs co-transcriptionally and Pol II elongation has been proposed to be coupled with successful capping, though a direct "capping checkpoint" has yet to be shown [85, 86]. Potential sensitivity of capping to Pol II GOF mutants is suggestive of either a defective checkpoint in Pol II mutant strains or the absence of one. We also observe correlations of reporter transcript half-life with expression levels in Pol II mutants, and with Pol II mutants' growth defects (**Figure 4**). Although we tested a single transcript, mRNA decay rate correlation with growth rate is consistent with recent findings [26, 27]. As growth efficiency can be directly connected the overall translation demand, our observation is consistent with the proposed 'feed-back' of gene expression control between transcription rate and mRNA decay occurring through alteration of overall translational rate, as mRNA decay happens co-translationally [87-89].

Here we extensively characterize a set of Pol II catalysis mutants for *in vivo* consequences. We show that altered Pol II catalysis affect Pol II occupancy, putative elongation, and reporter gene expression and decay rate *in vivo*. Notably, we interrogate two widely used elongation reporter systems, raising caveats about their use and interpretation. For use of nucleotide depleting drugs MPA or 6-AU, we constructed and tested an useful novel reporter system (*imd2*Δ::*HIS3*), which can be further utilized to

654 characterize or screen for new mutants that shift TSS usage downstream leading to constitutively
655 expression of *imd2*Δ*::HIS3*. Development of approaches allowing more direct determination of *in vivo*
656 elongation rate will bypass issues identified here. Recent advances in high-resolution microscopy have
657 enabled real-time observation of all transcription phases on endogenous genes using fluorescently
658 labeled proteins that bind to nascent transcript [90, 91]. This approach could be to address how any
659 number of variables might modulate elongation such as template sequence, RNA secondary structure
660 *etc*, and likely represents the next steps toward understanding transcription elongation and co-
661 transcriptional processes *in vivo*.
662

663 ## Acknowledgments

664 We thank Mary Bryk for providing bead beater for yeast cell breakage and UV cross-linker for blotting.
665 We are grateful to Jennifer Herman and Lanying Zeng for providing microscope time and training. We
666 thank Ry Young/Center for Phage Technology for use of Tecan plate reader. We thank Kaplan lab
667 members for critical reading of the manuscript and helpful comments. This work was supported by grant
668 R01GM097260 from the National Institutes of Health, National Institute for General Medical Sciences to
669 CDK, and grant A-1763 from the Welch Foundation to CDK.

670

671

References

1. Kaplan, C.D., *Basic mechanisms of RNA polymerase II activity and alteration of gene expression in Saccharomyces cerevisiae.* Biochim Biophys Acta, 2013. **1829**(1): p. 39-54.
2. Svetlov, V. and E. Nudler, *Basic mechanism of transcription by RNA polymerase II.* Biochim Biophys Acta, 2013. **1829**(1): p. 20-8.
3. Bentley, D.L., *Coupling mRNA processing with transcription in time and space.* Nat Rev Genet, 2014. **15**(3): p. 163-75.
4. Kaplan, C.D., et al., *Dissection of Pol II trigger loop function and Pol II activity-dependent control of start site selection in vivo.* PLoS Genet, 2012. **8**(4): p. e1002627.
5. Kaplan, C.D., K.M. Larsson, and R.D. Kornberg, *The RNA polymerase II trigger loop functions in substrate selection and is directly targeted by alpha-amanitin.* Mol Cell, 2008. **30**(5): p. 547-56.
6. Malagon, F., et al., *Mutations in the Saccharomyces cerevisiae RPB1 gene conferring hypersensitivity to 6-azauracil.* Genetics, 2006. **172**(4): p. 2201-9.
7. Wang, D., et al., *Structural basis of transcription: role of the trigger loop in substrate specificity and catalysis.* Cell, 2006. **127**(5): p. 941-54.
8. Kireeva, M.L., et al., *Transient reversal of RNA polymerase II active site closing controls fidelity of transcription elongation.* Mol Cell, 2008. **30**(5): p. 557-66.
9. Larson, M.H., et al., *Trigger loop dynamics mediate the balance between the transcriptional fidelity and speed of RNA polymerase II.* Proc Natl Acad Sci U S A, 2012. **109**(17): p. 6555-60.
10. Cabart, P., et al., *Activation and reactivation of the RNA polymerase II trigger loop for intrinsic RNA cleavage and catalysis.* Transcription, 2014. **5**(3): p. e28869.
11. Dangkulwanich, M., et al., *Complete dissection of transcription elongation reveals slow translocation of RNA polymerase II in a linear ratchet mechanism.* Elife, 2013. **2**: p. e00971.
12. Fong, N., et al., *Pre-mRNA splicing is facilitated by an optimal RNA polymerase II elongation rate.* Genes Dev, 2014. **28**(23): p. 2663-76.
13. Fusby, B., et al., *Coordination of RNA Polymerase II Pausing and 3' End Processing Factor Recruitment with Alternative Polyadenylation.* Mol Cell Biol, 2015. **36**(2): p. 295-303.
14. Braberg, H., et al., *From structure to systems: high-resolution, quantitative genetic analysis of RNA polymerase II.* Cell, 2013. **154**(4): p. 775-88.
15. Carrillo Oesterreich, F., et al., *Splicing of Nascent RNA Coincides with Intron Exit from RNA Polymerase II.* Cell, 2016. **165**(2): p. 372-81.
16. de la Mata, M., et al., *A slow RNA polymerase II affects alternative splicing in vivo.* Mol Cell, 2003. **12**(2): p. 525-32.
17. Jimeno-Gonzalez, S., et al., *The yeast 5'-3' exonuclease Rat1p functions during transcription elongation by RNA polymerase II.* Mol Cell, 2010. **37**(4): p. 580-7.
18. Hazelbaker, D.Z., et al., *Kinetic competition between RNA Polymerase II and Sen1-dependent transcription termination.* Mol Cell, 2013. **49**(1): p. 55-66.
19. Fong, N., et al., *Effects of Transcription Elongation Rate and Xrn2 Exonuclease Activity on RNA Polymerase II Termination Suggest Widespread Kinetic Competition.* Mol Cell, 2015. **60**(2): p. 256-67.
20. Zhang, H., F. Rigo, and H.G. Martinson, *Poly(A) Signal-Dependent Transcription Termination Occurs through a Conformational Change Mechanism that Does Not Require Cleavage at the Poly(A) Site.* Mol Cell, 2015. **59**(3): p. 437-48.
21. Braun, K.A., et al., *Phosphoproteomic analysis identifies proteins involved in transcription-coupled mRNA decay as targets of Snf1 signaling.* Sci Signal, 2014. **7**(333): p. ra64.
22. Braun, K.A. and E.T. Young, *Coupling mRNA synthesis and decay.* Mol Cell Biol, 2014. **34**(22): p. 4078-87.
23. Haimovich, G., et al., *Gene expression is circular: factors for mRNA degradation also foster mRNA synthesis.* Cell, 2013. **153**(5): p. 1000-11.
24. Sun, M., et al., *Global analysis of eukaryotic mRNA degradation reveals Xrn1-dependent buffering of transcript levels.* Mol Cell, 2013. **52**(1): p. 52-62.
25. Haimovich, G., et al., *The fate of the messenger is pre-determined: a new model for regulation of gene expression.* Biochim Biophys Acta, 2013. **1829**(6-7): p. 643-53.

26. Garcia-Martinez, J., et al., *The cellular growth rate controls overall mRNA turnover, and modulates either transcription or degradation rates of particular gene regulons.* Nucleic Acids Res, 2016. **44**(8): p. 3643-58.
27. Neymotin, B., V. Ettorre, and D. Gresham, *Global determinants of mRNA degradation rates in Saccharomyces cerevisiae.* bioRxiv, 2015.
28. Athanasiadou, N., et al., *Growth Rate-Dependent Global Amplification of Gene Expression.* bioRxiv, 2016.
29. Mason, P.B. and K. Struhl, *Distinction and relationship between elongation rate and processivity of RNA polymerase II in vivo.* Mol Cell, 2005. **17**(6): p. 831-40.
30. Hirayoshi, K. and J.T. Lis, *Nuclear run-on assays: assessing transcription by measuring density of engaged RNA polymerases.* Methods Enzymol, 1999. **304**: p. 351-62.
31. Garcia-Martinez, J., A. Aranda, and J.E. Perez-Ortin, *Genomic run-on evaluates transcription rates for all yeast genes and identifies gene regulatory mechanisms.* Mol Cell, 2004. **15**(2): p. 303-13.
32. Morillo-Huesca, M., M. Vanti, and S. Chavez, *A simple in vivo assay for measuring the efficiency of gene length-dependent processes in yeast mRNA biogenesis.* FEBS J, 2006. **273**(4): p. 756-69.
33. Ardehali, M.B. and J.T. Lis, *Tracking rates of transcription and splicing in vivo.* Nat Struct Mol Biol, 2009. **16**(11): p. 1123-4.
34. Archambault, J., et al., *Genetic interaction between transcription elongation factor TFIIS and RNA polymerase II.* Mol Cell Biol, 1992. **12**(9): p. 4142-52.
35. Sweeney, M.J., *Mycophenolic acid and its mechanism of action in cancer and psoriasis.* Jpn J Antibiot, 1977. **30 Suppl**: p. 85-92.
36. Powell, W. and D. Reines, *Mutations in the second largest subunit of RNA polymerase II cause 6-azauracil sensitivity in yeast and increased transcriptional arrest in vitro.* J Biol Chem, 1996. **271**(12): p. 6866-73.
37. Reines, D., *Use of RNA yeast polymerase II mutants in studying transcription elongation.* Methods Enzymol, 2003. **371**: p. 284-92.
38. Desmoucelles, C., et al., *Screening the yeast "disruptome" for mutants affecting resistance to the immunosuppressive drug, mycophenolic acid.* J Biol Chem, 2002. **277**(30): p. 27036-44.
39. Shaw, R.J. and D. Reines, *Saccharomyces cerevisiae transcription elongation mutants are defective in PUR5 induction in response to nucleotide depletion.* Mol Cell Biol, 2000. **20**(20): p. 7427-37.
40. Jenks, M.H., T.W. O'Rourke, and D. Reines, *Properties of an intergenic terminator and start site switch that regulate IMD2 transcription in yeast.* Mol Cell Biol, 2008. **28**(12): p. 3883-93.
41. Kuehner, J.N. and D.A. Brow, *Regulation of a eukaryotic gene by GTP-dependent start site selection and transcription attenuation.* Mol Cell, 2008. **31**(2): p. 201-11.
42. Riles, L., et al., *Large-scale screening of yeast mutants for sensitivity to the IMP dehydrogenase inhibitor 6-azauracil.* Yeast, 2004. **21**(3): p. 241-8.
43. Amberg, D.C., D.J. Burke, and J.N. Strathern, *Methods in Yeast Genetics: A Cold Spring Harbor Laboratory Course Manual, 2005 Edition (Cold Spring).* 2005.
44. Lenstra, T.L. and F.C. Holstege, *The discrepancy between chromatin factor location and effect.* Nucleus, 2012. **3**(3): p. 213-9.
45. Kaplan, C.D., M.J. Holland, and F. Winston, *Interaction between transcription elongation factors and mRNA 3'-end formation at the Saccharomyces cerevisiae GAL10-GAL7 locus.* J Biol Chem, 2005. **280**(2): p. 913-22.
46. Livak, K.J. and T.D. Schmittgen, *Analysis of relative gene expression data using real-time quantitative PCR and the 2(-Delta Delta C(T)) Method.* Methods, 2001. **25**(4): p. 402-8.
47. Schmitt, M.E., T.A. Brown, and B.L. Trumpower, *A rapid and simple method for preparation of RNA from Saccharomyces cerevisiae.* Nucleic Acids Res, 1990. **18**(10): p. 3091-2.
48. Marquardt, S., D.Z. Hazelbaker, and S. Buratowski, *Distinct RNA degradation pathways and 3' extensions of yeast non-coding RNA species.* Transcription, 2011. **2**(3): p. 145-154.
49. Ranish, J.A. and S. Hahn, *The yeast general transcription factor TFIIA is composed of two polypeptide subunits.* J Biol Chem, 1991. **266**(29): p. 19320-7.

50. Miermont, A., et al., *Severe osmotic compression triggers a slowdown of intracellular signaling, which can be explained by molecular crowding.* Proc Natl Acad Sci U S A, 2013. **110**(14): p. 5725-30.
51. Jin, H. and C.D. Kaplan, *Relationships of RNA polymerase II genetic interactors to transcription start site usage defects and growth in Saccharomyces cerevisiae.* G3 (Bethesda), 2014. **5**(1): p. 21-33.
52. Danko, C.G., et al., *Signaling pathways differentially affect RNA polymerase II initiation, pausing, and elongation rate in cells.* Mol Cell, 2013. **50**(2): p. 212-22.
53. Jonkers, I., H. Kwak, and J.T. Lis, *Genome-wide dynamics of Pol II elongation and its interplay with promoter proximal pausing, chromatin, and exons.* Elife, 2014. **3**: p. e02407.
54. Veloso, A., et al., *Rate of elongation by RNA polymerase II is associated with specific gene features and epigenetic modifications.* Genome Res, 2014. **24**(6): p. 896-905.
55. Miguel, A., et al., *External conditions inversely change the RNA polymerase II elongation rate and density in yeast.* Biochim Biophys Acta, 2013. **1829**(11): p. 1248-55.
56. Pelechano, V., et al., *Regulon-specific control of transcription elongation across the yeast genome.* PLoS Genet, 2009. **5**(8): p. e1000614.
57. Barnes, C.O., et al., *Crystal Structure of a Transcribing RNA Polymerase II Complex Reveals a Complete Transcription Bubble.* Mol Cell, 2015. **59**(2): p. 258-69.
58. Millan-Zambrano, G., et al., *The prefoldin complex regulates chromatin dynamics during transcription elongation.* PLoS Genet, 2013. **9**(9): p. e1003776.
59. Kim, M., et al., *The yeast Rat1 exonuclease promotes transcription termination by RNA polymerase II.* Nature, 2004. **432**(7016): p. 517-22.
60. Luo, W., A.W. Johnson, and D.L. Bentley, *The role of Rat1 in coupling mRNA 3'-end processing to transcription termination: implications for a unified allosteric-torpedo model.* Genes Dev, 2006. **20**(8): p. 954-65.
61. Jimeno-Gonzalez, S., et al., *Rat1p maintains RNA polymerase II CTD phosphorylation balance.* RNA, 2014. **20**(4): p. 551-8.
62. Jiao, X., et al., *Identification of a quality-control mechanism for mRNA 5'-end capping.* Nature, 2010. **467**(7315): p. 608-11.
63. Chang, J.H., et al., *Dxo1 is a new type of eukaryotic enzyme with both decapping and 5'-3' exoribonuclease activity.* Nat Struct Mol Biol, 2012. **19**(10): p. 1011-7.
64. Mason, P.B. and K. Struhl, *The FACT complex travels with elongating RNA polymerase II and is important for the fidelity of transcriptional initiation in vivo.* Mol Cell Biol, 2003. **23**(22): p. 8323-33.
65. Chen, H., et al., *Genome-wide study of mRNA degradation and transcript elongation in Escherichia coli.* Mol Syst Biol, 2015. **11**(5): p. 808.
66. Nehlin, J.O., M. Carlberg, and H. Ronne, *Control of yeast GAL genes by MIG1 repressor: a transcriptional cascade in the glucose response.* EMBO J, 1991. **10**(11): p. 3373-7.
67. Gancedo, J.M., *Yeast carbon catabolite repression.* Microbiol Mol Biol Rev, 1998. **62**(2): p. 334-61.
68. De Vit, M.J., J.A. Waddle, and M. Johnston, *Regulated nuclear translocation of the Mig1 glucose repressor.* Mol Biol Cell, 1997. **8**(8): p. 1603-18.
69. Shaw, R.J., et al., *Regulation of an IMP dehydrogenase gene and its overexpression in drug-sensitive transcription elongation mutants of yeast.* J Biol Chem, 2001. **276**(35): p. 32905-16.
70. Hyle, J.W., R.J. Shaw, and D. Reines, *Functional distinctions between IMP dehydrogenase genes in providing mycophenolate resistance and guanine prototrophy to yeast.* J Biol Chem, 2003. **278**(31): p. 28470-8.
71. Jenks, M.H. and D. Reines, *Dissection of the molecular basis of mycophenolate resistance in Saccharomyces cerevisiae.* Yeast, 2005. **22**(15): p. 1181-90.
72. Exinger, F. and F. Lacroute, *6-Azauracil inhibition of GTP biosynthesis in Saccharomyces cerevisiae.* Curr Genet, 1992. **22**(1): p. 9-11.
73. Hartzog, G.A., et al., *Evidence that Spt4, Spt5, and Spt6 control transcription elongation by RNA polymerase II in Saccharomyces cerevisiae.* Genes Dev, 1998. **12**(3): p. 357-69.
74. Gaillard, H., et al., *Genome-wide analysis of factors affecting transcription elongation and DNA repair: a new role for PAF and Ccr4-not in transcription-coupled repair.* PLoS Genet, 2009. **5**(2): p. e1000364.

75. Gaur, N.A., et al., *Vps factors are required for efficient transcription elongation in budding yeast.* Genetics, 2013. **193**(3): p. 829-51.
76. Squazzo, S.L., et al., *The Paf1 complex physically and functionally associates with transcription elongation factors in vivo.* EMBO J, 2002. **21**(7): p. 1764-74.
77. Denis, C.L., et al., *Genetic evidence supports a role for the yeast CCR4-NOT complex in transcriptional elongation.* Genetics, 2001. **158**(2): p. 627-34.
78. Davis, C.A. and M. Ares, Jr., *Accumulation of unstable promoter-associated transcripts upon loss of the nuclear exosome subunit Rrp6p in Saccharomyces cerevisiae.* Proc Natl Acad Sci U S A, 2006. **103**(9): p. 3262-7.
79. Steinmetz, E.J., et al., *Genome-wide distribution of yeast RNA polymerase II and its control by Sen1 helicase.* Mol Cell, 2006. **24**(5): p. 735-46.
80. Canadell, D., et al., *Impact of high pH stress on yeast gene expression: A comprehensive analysis of mRNA turnover during stress responses.* Biochim Biophys Acta, 2015. **1849**(6): p. 653-64.
81. Howard, S.C., et al., *The Ras/PKA signaling pathway of Saccharomyces cerevisiae exhibits a functional interaction with the Sin4p complex of the RNA polymerase II holoenzyme.* Genetics, 2001. **159**(1): p. 77-89.
82. Howard, S.C., A. Hester, and P.K. Herman, *The Ras/PKA signaling pathway may control RNA polymerase II elongation via the Spt4p/Spt5p complex in Saccharomyces cerevisiae.* Genetics, 2003. **165**(3): p. 1059-70.
83. Darby, M.M., et al., *The Saccharomyces cerevisiae Nrd1-Nab3 transcription termination pathway acts in opposition to Ras signaling and mediates response to nutrient depletion.* Mol Cell Biol, 2012. **32**(10): p. 1762-75.
84. Cui, P., et al., *Relationships Between RNA Polymerase II Activity and Spt Elongation Factors to Spt- Phenotype and Growth in Saccharomyces cerevisiae.* G3 (Bethesda), 2016.
85. Rasmussen, E.B. and J.T. Lis, *In vivo transcriptional pausing and cap formation on three Drosophila heat shock genes.* Proc Natl Acad Sci U S A, 1993. **90**(17): p. 7923-7.
86. Glover-Cutter, K., et al., *RNA polymerase II pauses and associates with pre-mRNA processing factors at both ends of genes.* Nat Struct Mol Biol, 2008. **15**(1): p. 71-8.
87. Hu, W., et al., *Nonsense-mediated mRNA decapping occurs on polyribosomes in Saccharomyces cerevisiae.* Nat Struct Mol Biol, 2010. **17**(2): p. 244-7.
88. Hu, W., et al., *Co-translational mRNA decay in Saccharomyces cerevisiae.* Nature, 2009. **461**(7261): p. 225-9.
89. Pelechano, V., W. Wei, and L.M. Steinmetz, *Widespread Co-translational RNA Decay Reveals Ribosome Dynamics.* Cell, 2015. **161**(6): p. 1400-12.
90. Larson, D.R., et al., *Real-time observation of transcription initiation and elongation on an endogenous yeast gene.* Science, 2011. **332**(6028): p. 475-8.
91. Hocine, S., et al., *Single-molecule analysis of gene expression using two-color RNA labeling in live yeast.* Nat Methods, 2013. **10**(2): p. 119-21.

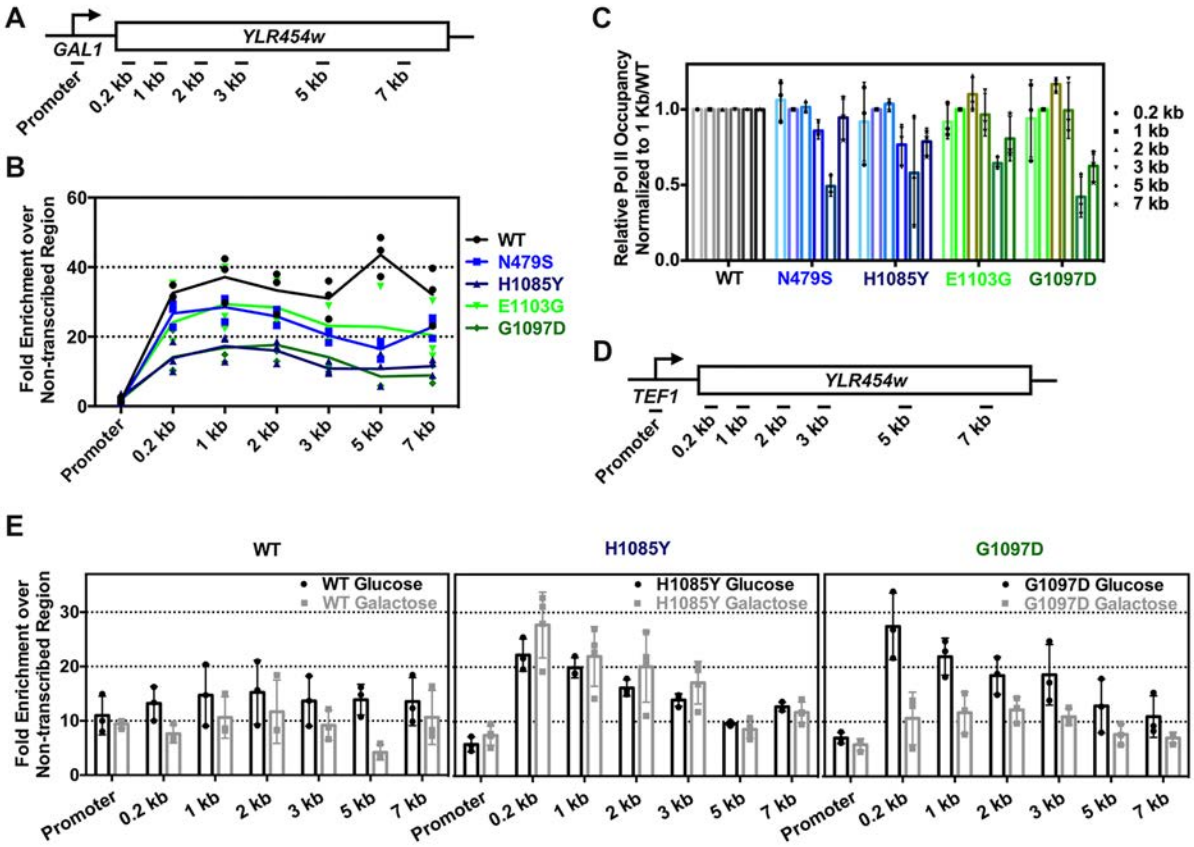

876

877 **Figure1. Pol II catalytic mutants alter Pol II occupancy and apparent processivity.** (A) Schematic of
878 the galactose inducible reporter *GAL1p*::*YLR454w* annotated with positions of PCR amplicons used for
879 ChIP experiments. Promoter amplicon derived from primers specific to the *kanmx::GAL1p* integrated
880 promoter. (B) Steady-state Pol II occupancy at *GAL1p*::*YLR454w* for WT and Pol II catalytic mutants
881 under galactose induction. Green and blue color-coding is used to annotate GOF and LOF mutants,
882 respectively. This color-coding is used throughout. (C) Apparent Pol II processivity defects determined
883 for each mutant by normalizing mutant ChIP signal to signal at 1kb followed by normalization to WT. (D)
884 Schematic of constitutively expressed reporter gene *TEF1p*::*YLR454w* annotated with positions of PCR
885 amplicons used for ChIP experiments. Promoter amplicon derived from primers specific to the
886 *kanmx::TEF1p* integrated promoter. (E) Comparison of steady-state Pol II occupancy at
887 *TEF1p*::*YLR454w* for WT and Pol II catalytic mutants grown in galactose- or glucose-containing medium.
888 Individual data points from at least three biological repeats are shown with bars showing average +/- the
889 standard deviation of the mean.

890

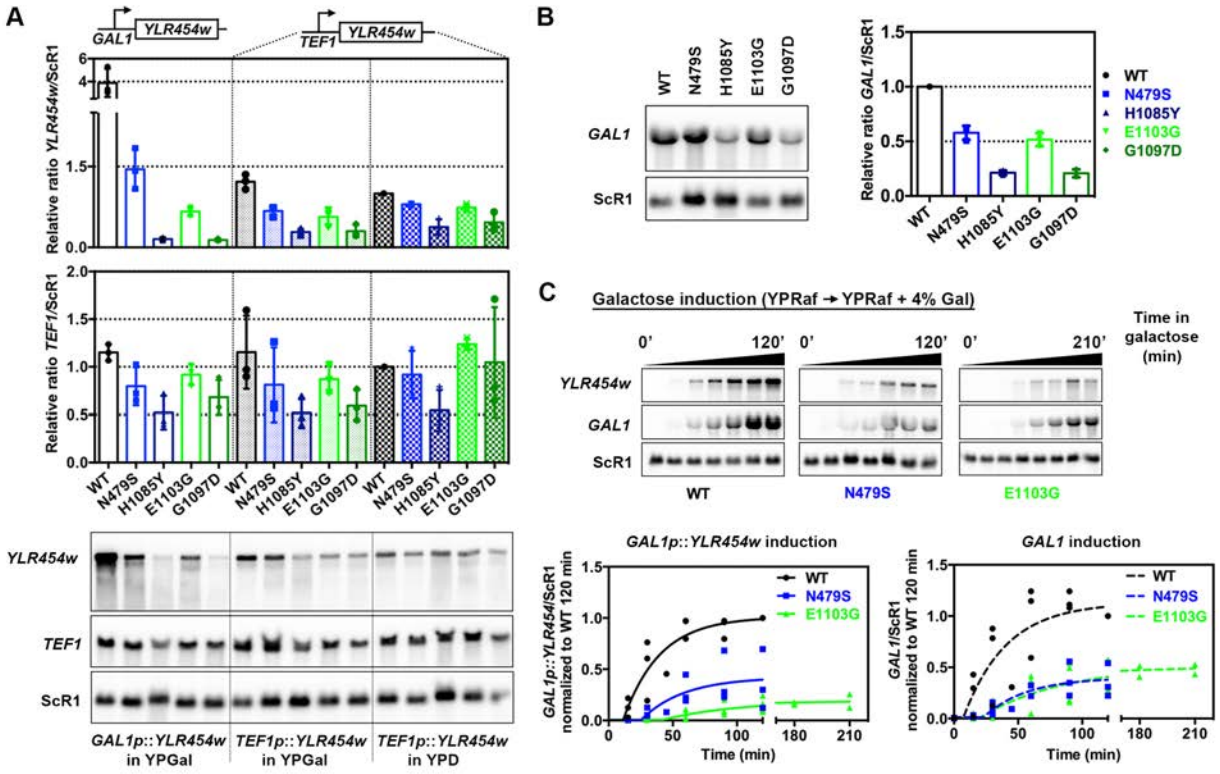

Figure 2. Pol II catalytic mutants affect in vivo gene expression. (A) Steady-state RNA levels of reporter genes used for Pol II occupancy experiments (*GAL1p*::*YLR454w* and *TEF1p*::*YLR454w*) and endogenous *TEF1* levels from cells grown in galactose- or glucose-containing medium as indicated. Values normalized to WT *TEF1p*::*YLR454w* expression level in YPD. Individual data points from at least three biological repeats are shown with bars indicating average +/- standard deviation of the mean. (B) Endogenous *GAL1* mRNA levels in WT and Pol II catalytic mutant strains. Values normalized to WT *GAL1* mRNA level. Error bars as in A. (C) Time courses showing induction of *GAL1p*::*YLR454w* and endogenous *GAL1* mRNA in WT and Pol II catalytic mutants. Overnight grown cells were inoculated into fresh YPRaf medium and grown until mid-log phase at 30˚C, subsequently 4% galactose (final) was added to induce *GAL* gene expression. RNAs isolated prior (time 0) and after galactose addition were used for Northern blotting to determine accumulation of mature *GAL1p*::*YLR454w* and endogenous *GAL1*. Data normalized to WT 120 min value and plotted using non-linear regression using GraphPad Prism. Individual data points from at least three biological repeats are shown.

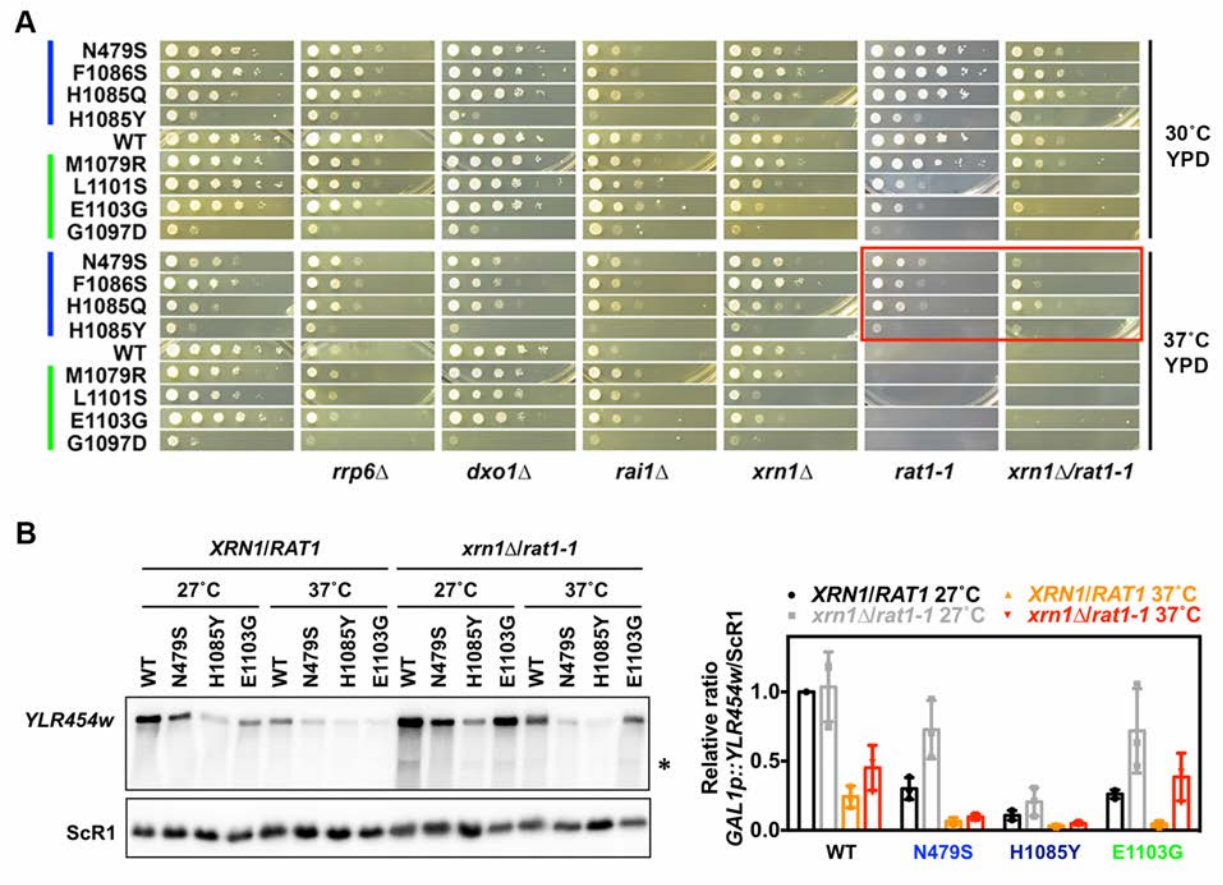

Figure 3. Allele-specific genetic interactions between Pol II catalytic mutants and pre-mRNA processing factors. (A) 10-fold serial dilutions of saturated cultures of Pol II catalytic mutants alone or in combination with pre-mRNA processing factor mutants plated on YPD for comparison of growth at 30˚C and 37˚C. GOF and LOF mutants are annotated with green and blue bars, respectively. Suppression of *rat1-1* lethality at restrictive temperature is highlighted in red box. (B) (Left) Representative gel showing *GAL1p*::*YLR454w* reporter expression level in Pol II catalytic mutants in WT and *xrn1*Δ/*rat1-1* mutant background. Overnight grown cells inoculated in fresh YPRaf/Gal media to amplify until mid-log at permissive temperature (27˚C) then shifted to restrictive temperature (37˚C) to inactivate Rat1-1p. RNAs isolated from the half of the culture before shifting temperature used as 27˚C sample. The other half was washed and resuspended in pre-warmed YPRaf/Gal media to grow for another 2 hrs at 37˚C to isolate 37˚C sample for Northern blotting. Asterisk indicates internal cryptic transcript stabilized *xrn1*Δ/*rat1-1* mutant background. (Right) Quantification of *xrn1*Δ/*rat1-1* effects. Values were normalized to WT *GAL1*p::*YLR454w* mRNA level (*XRN1*/*RAT1*) at 27˚C. Data shown are average of three biological repeats with error bars representing standard deviation of the mean.

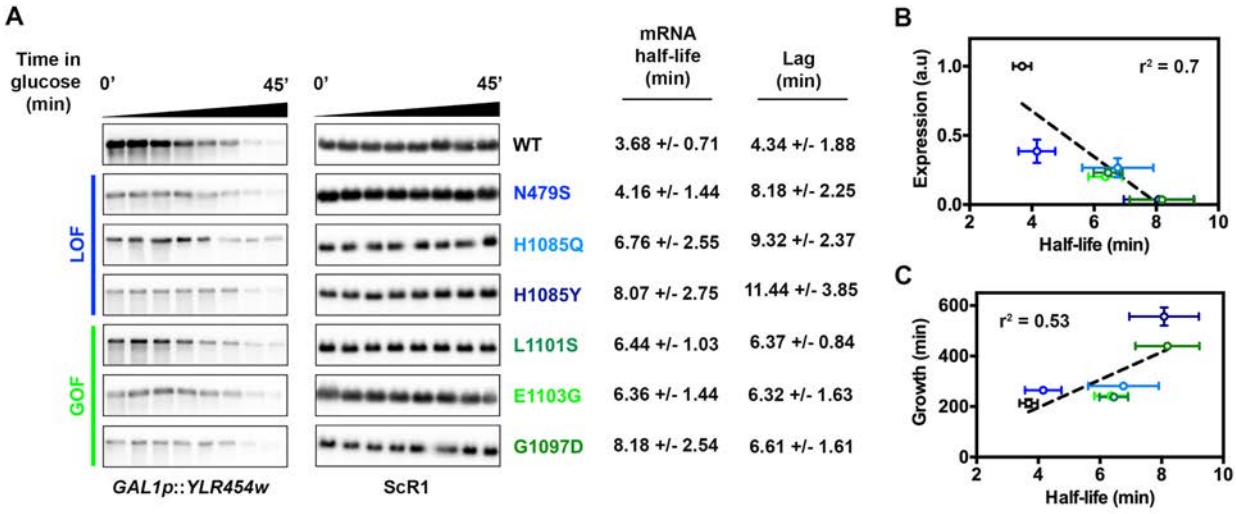

923

924 **Figure 4. Pol II catalytic mutants alter mRNA half-life of the reporter.** (A) Representative blots
925 showing *GAL1p*::*YLR454w* mRNA decay, determined by glucose shut off. Overnight grown cells
926 inoculated in fresh YPGal media to grow till mid-log at 30˚C. RNAs isolated from pre-glucose addition
927 (time 0) and post-glucose addition time points used for Northern blotting. mRNA half-lives and lags were
928 determined using plateau followed by one-phase decay curve fitting in GraphPad Prism (see
929 **Supplementary Figure 2A**). Values indicate average of a minimum of five repeats with error bars
930 representing standard deviation of the mean. (B and C) Correlation of *GAL1p*::*YLR454w* half-life in
931 different mutants with the expression level (**Figure 2A** and **Supplementary Figure 2I**) and with the
932 mutants' growth defects (**Supplementary Figure 2H**) determined by linear regression using GraphPad
933 Prism.

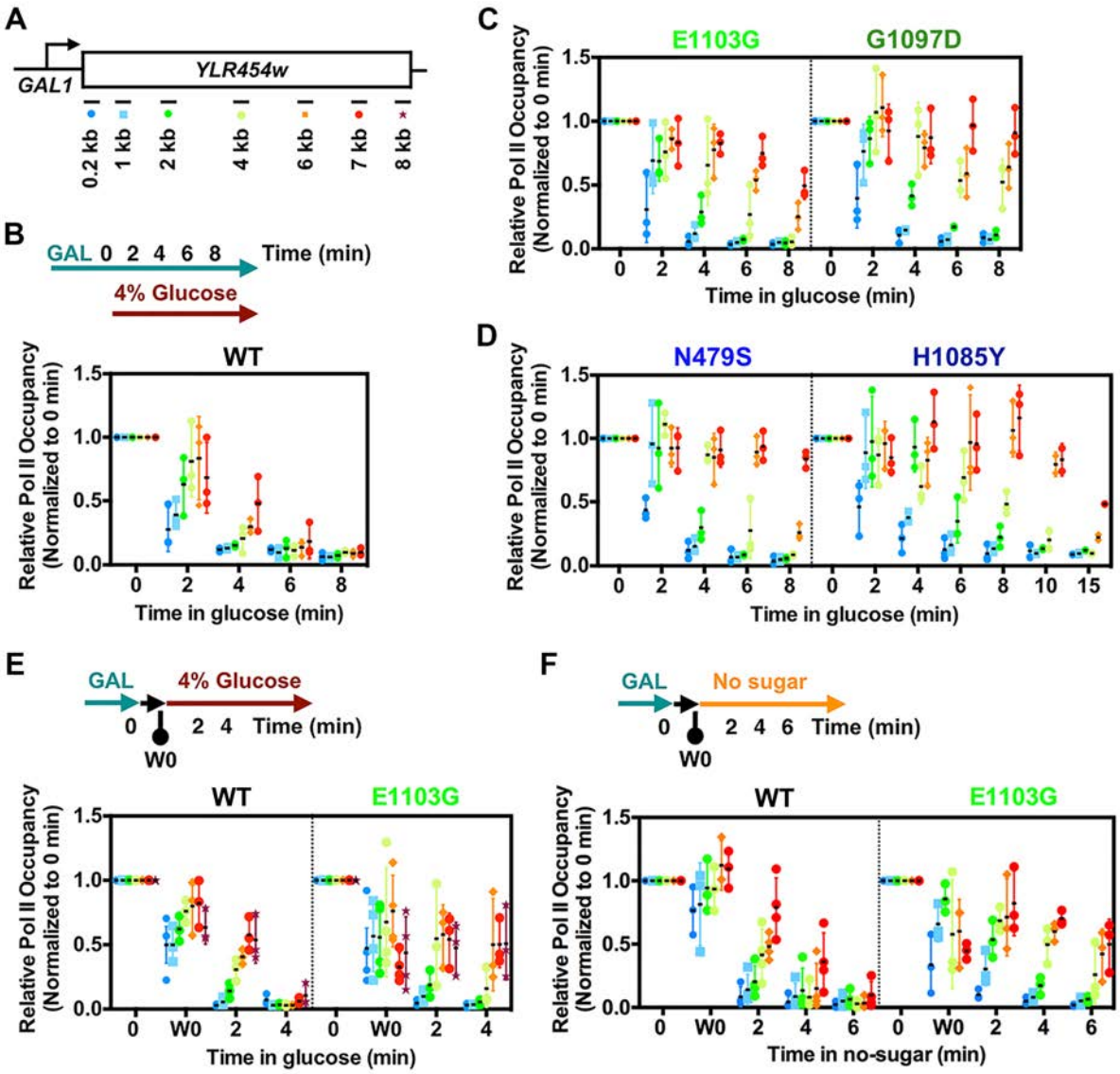

Figure 5. Pol II catalytic mutants show slower in vivo elongation rate in glucose shut off assay. (A) Schematic of the *GAL1p*::*YLR454w* with positions of PCR amplicons used for ChIP experiments. (B) Schematic of the regular glucose shut off experiment used in B-D. *In vivo* apparent elongation rate for WT, fast (C; E1103G and G1097D) and slow (D; N479S and H1085Y) catalytic mutants determined by ChIP upon glucose shut off of transcription by direct addition of 4% glucose (final) to the mid-log grown culture in YPGal at 30˚C. Scatter plot data indicate values normalized to pre-glucose addition (0 min) and error bars represent standard deviation of the mean for at least three independent experiments. For H1085Y, longer time point (10 and 15 min) values obtained from two repeats, with error bars indicating the range of the two experiments. (E) Glucose shut off assay to compare apparent *in vivo* elongation rate between WT and fast catalytic mutant (E1103G) following Hazelbaker et al., protocol [18]. Pre-glucose sample (0 min) was isolated as described in Figure 5A; subsequently cells were washed in synthetic complete media lacking carbon source and inoculated in YPD (4% dextrose) to shut off the transcription. One wash 0 (W0 min) sample was isolated after the washing and before shut off to determine the effect of washing. Values normalized to pre-glucose addition (0 min) and error bars represent standard deviation of the mean of at least three independent repeats. (F) Galactose depletion to determine apparent elongation rate in WT and fast catalytic mutant (E1103G). Pre-glucose and (0 min) and wash 0 (W0 min) samples were taken as described in Fig 5G, followed by inoculation of cells

952 into synthetic media lacking any carbon to incur transcriptional shutoff in absence of any sugar. Values
953 normalized to pre-glucose addition (0 min) and error bars represent standard deviation of the mean for at
954 least three independent repeats.

955

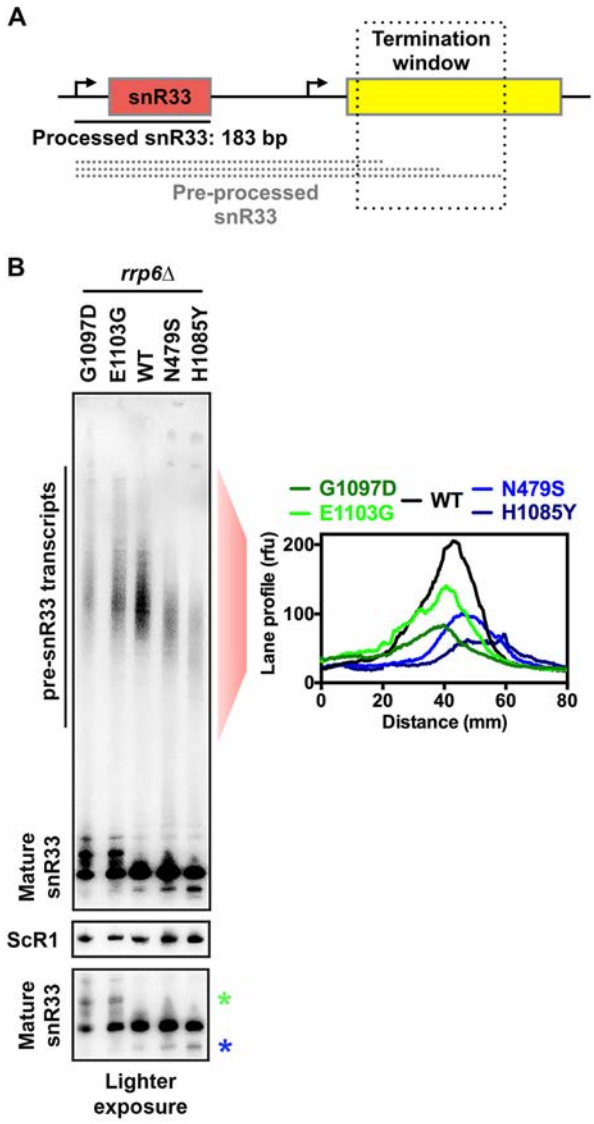

Figure 6. Mapping of termination window for preprocessed *SNR33* in WT and Pol II catalytic mutants. (A) Schematic of the snR33 termination window. (B) Northern blotting of *SNR33* for WT, slow (N479S and H1085Y) and fast (E1103G and G1097D) catalytic mutants containing deletion of the nuclear exosome subunit gene *RRP6.* Pol III transcript ScR1 used as loading control. Average densitometric values of indicated lanes from three independent repeats are presented in the graph. A lighter exposure of the mature snR33 full-length transcript shows alternative longer (green asterisk) and shorter (blue asterisk) products for GOF and LOF mutants, respectively, and are proposed due to shifts in TSS usage.

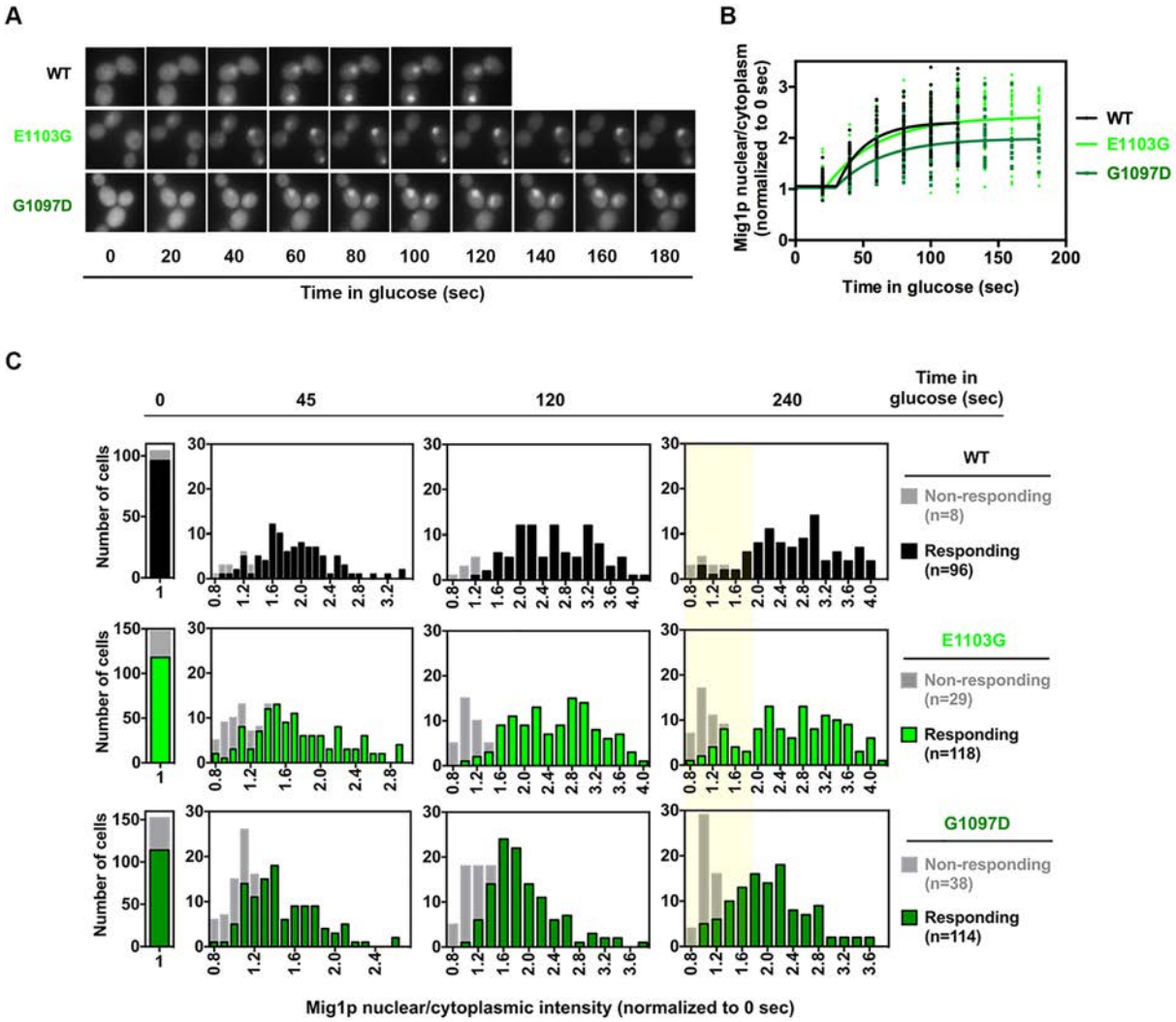

966

967 **Figure 7. Mig1 nuclear translocation is aberrant in Pol II GOF mutants E1103G and G1097D.** (A)
968 Representative images of nuclear localization of Mig1p-GFP in WT and catalytic mutants (E1103G and
969 G1097D) upon glucose (4% final) addition. Overnight grown cells were inoculated into fresh synthetic
970 complete medium containing galactose (SC-2% Gal) and grown until mid-log phase at 30˚C. Pre-glucose
971 repression samples used as time 0 (t0), followed by replacing the medium with SC-2% Gal + 4% glucose
972 to induce repression. (B) Mig1p nuclear localization kinetics. Normalized (to pre-glucose treatment; t0)
973 data from glucose-responding cells (n>35) plotted using non-linear regression in GraphPad Prism. (C)
974 Histograms of Mig1p nuclear localization show the distribution of nuclear Mig1p fluorescence
975 (normalized to t0) intensity over indicated time points. Cells that do not show any traces of fluorescence
976 accumulation are designated as non-responding cells (see methods for quantification details).
977 Highlighted area indicates population of cells that are either non-responding or responding cells with
978 decreased Mig1p nuclear localization.

979

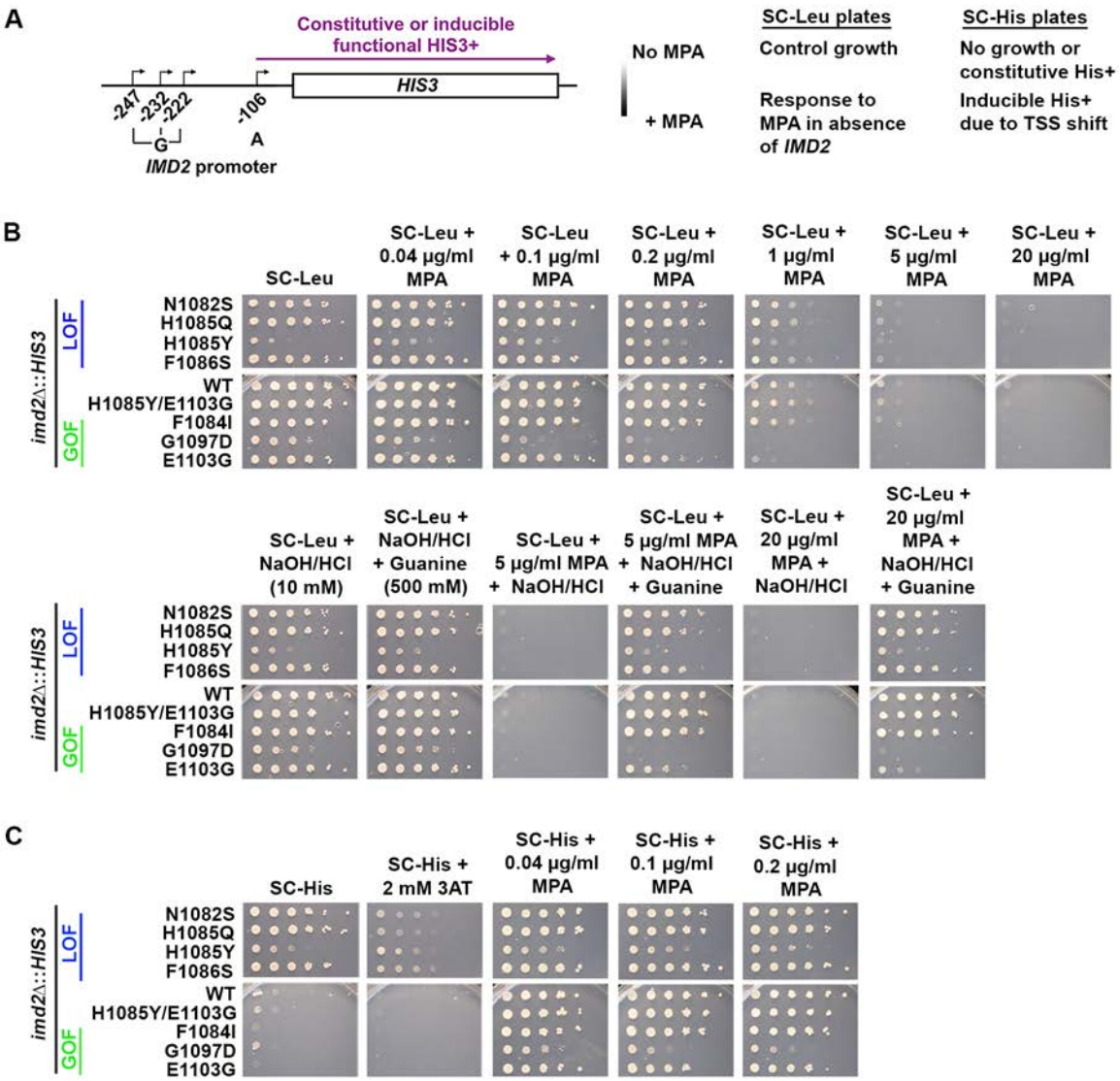

Figure 8. Pol II catalytic mutants defective of *IMD2* transcription do not abolish GTP sensing. (A) Schematic of the *imd2*Δ::*HIS3* construct and expected phenotype upon MPA treatment in synthetic medium lacking leucine or histidine. (B) 10-fold serial dilutions of saturated cultures of Pol II catalytic mutants plated on synthetic medium lacking leucine for comparison of growth in various concentration of MPA treatment at 30˚C. All strains lack endogenous *IMD2* ORF, which is replaced with *HIS3* (*imd2*Δ::*HIS3*), hence rendering them highly sensitive to MPA treatment. (C) 10-fold serial dilutions of saturated cultures of Pol II catalytic mutants plated on synthetic medium lacking histidine for comparison of growth in various concentration of MPA treatment at 30˚C.

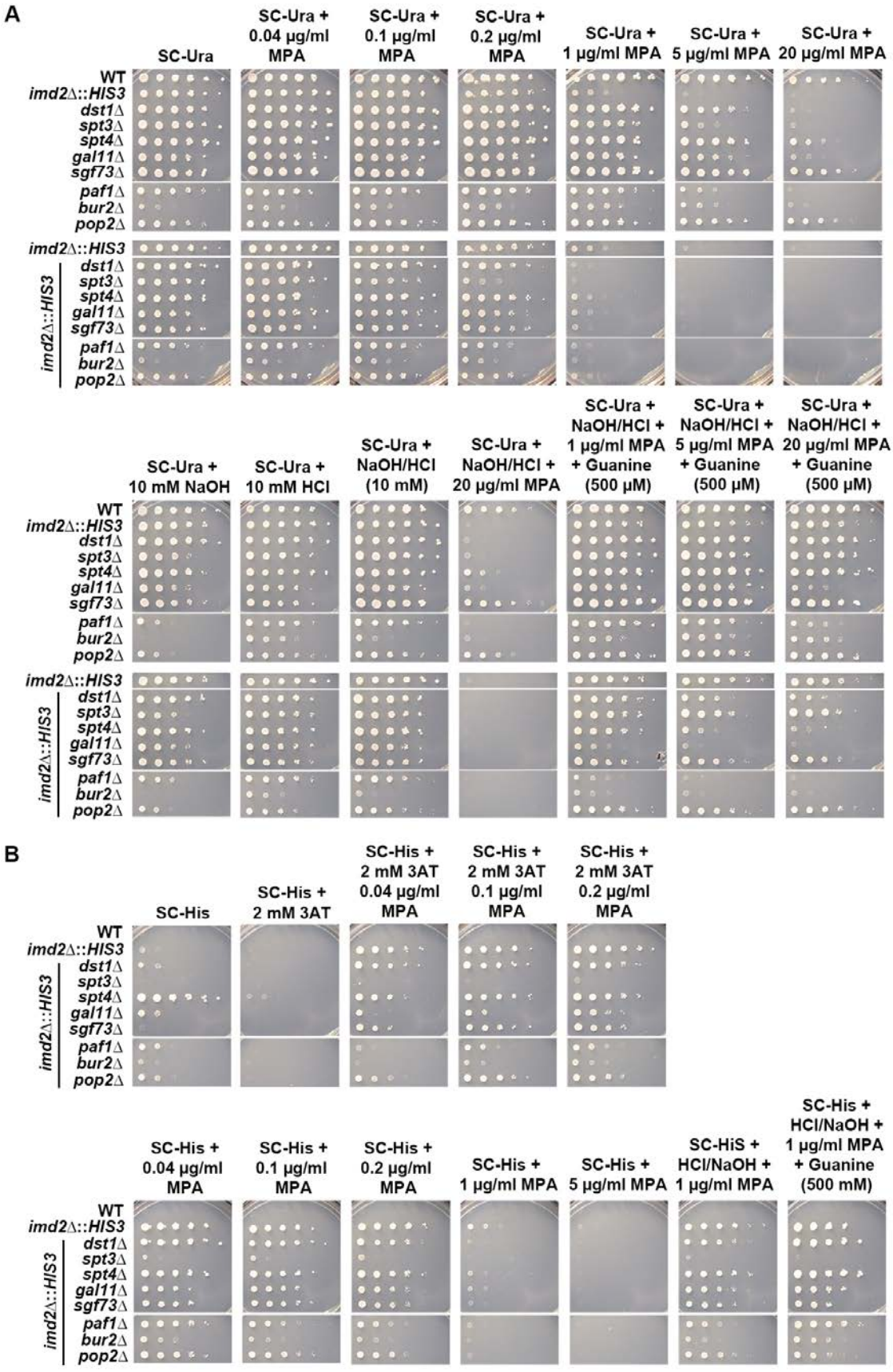

Figure 9. Transcription related factor mutants respond similar way to WT upon MPA treatment in absence of endogenous *IMD2*. (A) 10-fold serial dilutions of saturated cultures of indicated factor mutants plated on synthetic medium lacking uracil for comparison of growth in various concentration of MPA treatment at 30˚C. Upper and lower panel contains factor mutant strains with and without endogenous *IMD2* ORF (*imd2*Δ::*HIS3*), respectively. For convenience of comparison, spots of WT strain with *imd2*Δ::*HIS3* (second on the upper panel) is repeatedly presented next to factor mutants with *imd2*Δ::*HIS3* (top of the lower panel). (B) 10-fold serial dilutions of saturated cultures of indicated factor mutants plated on synthetic medium lacking histidine for comparison of growth in various concentration of MPA treatment at 30˚C.

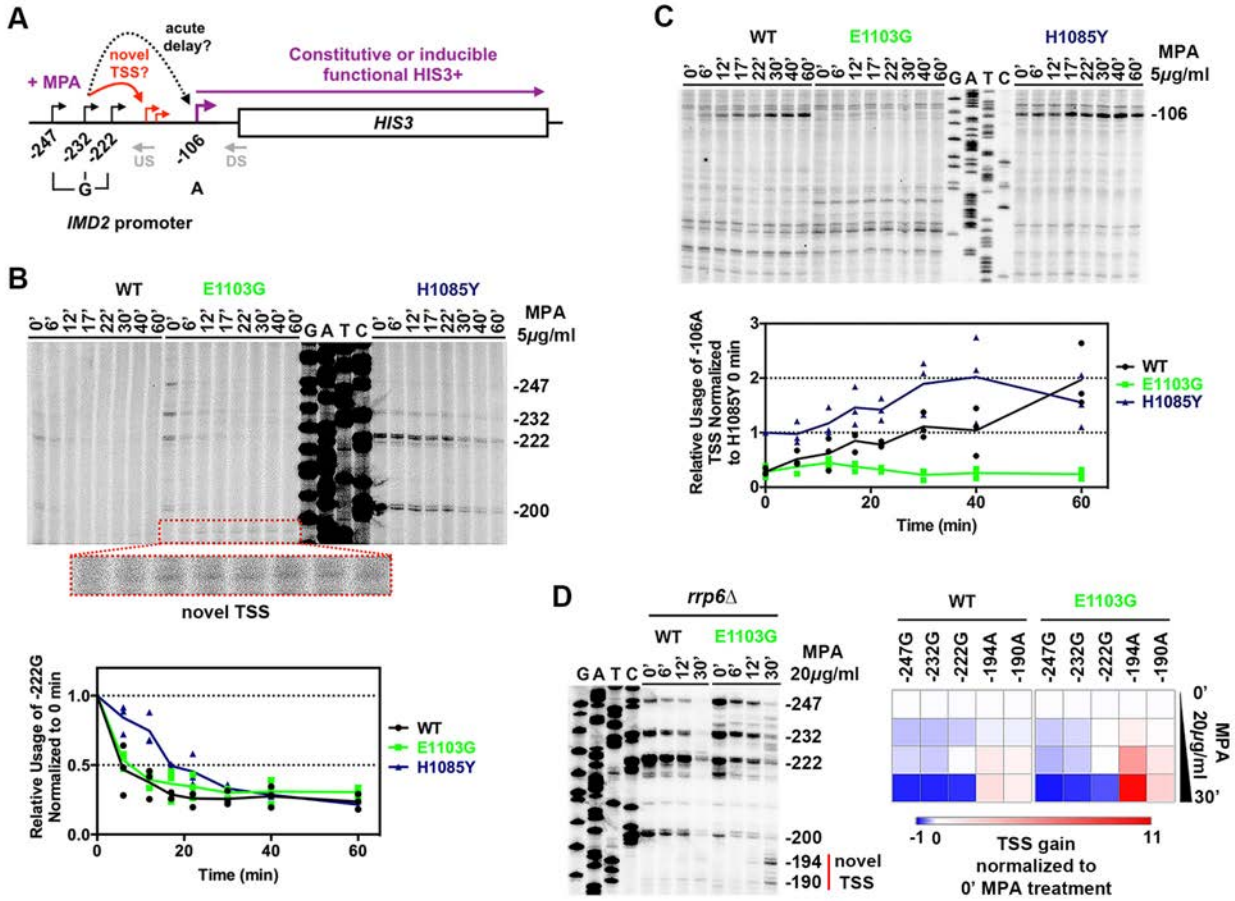

Figure 10. Pol II catalytic mutants do not abolish response to GTP depletion. (A) Schematic of the *imd2*Δ::*HIS3* construct used to determine WT and Pol II catalytic mutants' response to nucleotide depletion in absence of endogenous *IMD2*. Architecture of the *IMD2* promoter indicating the upstream 'G' start sites that are used in under normal GTP levels to produce a non-functional *IMD2* cryptic unstable transcript (CUT). Downstream 106 'A' is used upon presumptive GTP-depletion in presence of MPA, producing a functional transcript that confers MPA resistance if *IMD2* ORF is present. Slow catalytic mutants constitutively show use of both upstream and downstream start sites. Gray "US" (Upstream) and "DS" (Downstream) indicate positions of primers used for primer extension experiments. Two models for MPA-sensitivity of Pol II mutants are shown: TSS shift to inappropriate novel TSS, or acute delay in shift to appropriate TSS. (B) Time courses showing the usage of upstream 'G' sites upon MPA treatment (US primer used for PE). Cells grown to mid-log phase in synthetic complete media at 30˚C were treated with MPA (5 μg/mL final concentration) and RNAs isolated at indicated time points. Pre-treatment sample used for time 0. Graph shows the relative usage of -222G site for WT and mutants upon MPA treatment normalized to 0 min (no-treatment). (C) Same RNAs from Figure 8B used for PE experiment with DS primer to determine the usage of downstream 'A' sites upon MPA treatment. Graph shows the relative gain of -106A site for WT and mutants upon MPA treatment normalized to H1085Y 0 min (no-treatment), which is used constitutively. (D) Fast catalytic mutants gradually lose upstream 'G' sites and shift TSS usage to novel 'A' sites (putatively 194A and 190A) in response to nucleotide depletion. Usage of these sites likely produce non-functional CUTs shown to be stabilized here by the deletion of exosome subunit gene *RRP6*. Heat map represents the average loss/gain of indicated TSS upon MPA treatment obtained from three independent repeats (see **Supplementary Fig 6**).